

# Advances in Imaging Chest Tuberculosis: Blurring of Differences Between Children and Adults

Savvas Andronikou, MBBCh, FCRad, FRCR, PhD<sup>a,b,\*</sup>,  
Filip M. Vanhoenacker, MD, PhD<sup>c,d</sup>,  
Adelard I. De Backer, MD, PhD<sup>e</sup>

## KEYWORDS

- Imaging • Children and adults • Chest
- Radiological classification

## ROLE OF IMAGING

If there was a reliable, cheap, and fast clinical test to diagnose tuberculosis (TB), then imaging would probably be relegated to looking for complications and providing alternative diagnoses in nonresponders. As things stand however, current clinical signs and tests for diagnosing TB do not do the job well enough, cheaply enough, or quickly enough and imaging continues to play a role in the diagnosis and management of TB. Sputum microscopy (and culture) is specific for diagnosis and may be widely available, however, a large proportion of patients, and children in particular, are found to be smear-negative. Imaging remains useful for diagnosis, detection of complications, monitoring response to therapy, and for evaluating outcome.

Diagnosis using imaging is difficult for several reasons: changing patterns of disease; effects of human immunodeficiency virus (HIV) coinfection and AIDS<sup>1</sup>; inability to identify drug resistance; nonspecific radiographic signs<sup>1</sup>; subjective interpretation with inter- and intraobserver variability

of readers<sup>1-3</sup>; possibility of a normal radiograph<sup>1</sup>; problems distinguishing active from inactive disease and infection from disease; imaging is also expensive and often unavailable; radiography is subject to variable quality in technique.

## HAS OUR THINKING CHANGED?

The traditional classification of TB into primary and postprimary (reactivation TB) should be avoided<sup>4</sup> as the pathologic differences between these and the corresponding classic imaging patterns characterizing disease in adults and children have blurred. The age-related distinction has changed because primary infection can occur at any age (especially in countries with low TB incidence)<sup>5</sup>; because of exogenous reinfection in endemic areas<sup>4,6-8</sup>; cavitation occurring within 6 months of initial infection (reducing its status as indicator of reactivation),<sup>4</sup> and because HIV infection results in atypical patterns of disease. A radiological classification of disease is more appropriate.

<sup>a</sup> Diagnostic Imaging Working Group, Medecins Sans Frontiers, Plantage middenlaan 14, Amsterdam, The Netherlands

<sup>b</sup> Department of Radiology, University of Cape Town, Anzio Road, Observatory, Cape Town, South Africa

<sup>c</sup> Department of Radiology, Sint-Maarten Hospital, Duffel-Mechelen, Belgium

<sup>d</sup> University Hospital Antwerp, UZA, University of Antwerp, Wilrijkstraat, 10, B-2650, Edegem, Belgium

<sup>e</sup> Department of Radiology, Sint-Lucas Hospital, Groenebriel, 1, B-9000, Ghent, Belgium

\* Corresponding author. Department of Radiology, University of Cape Town, Anzio Road, Observatory, Cape Town, South Africa.

E-mail address: docsav@mweb.co.za (S. Andronikou).

## RADIOLOGICAL CLASSIFICATION

- Lymph node TB (gangliopulmonary TB)
- Air-space parenchymal TB (consolidation)
- Tuberculoma
- Miliary TB
- Cavities
- Pleural TB
- Fibrosis and destruction

## ADDITIONAL FACTORS

Various situations requires different information from the image reader and in turn require more information to be supplied to the reader for an insightful and meaningful interpretation: drug resistance requires the reader to give information on the presence and location of cavities and progression or stability of radiographic findings; HIV coinfection requires a different level of suspicion and a specific differential diagnosis depending on the combination of radiographic findings and clinical information (eg, CD4 count); complications of TB should be looked for, depending on the clinical presentation and previous imaging findings; treatment centers require comment on activity and whether findings indicate infection or disease, which affects management.

## NATIONAL OR PROGRAM POLICY

The role, influence, and level of imaging depend on various factors within each country, project, and setting, and may even vary according to current universal attitude or personal experience of individuals. These variations are influenced by the incidence of TB in a community or the world at large, geography, socioeconomic factors, the age of patients, HIV coinfection, drug resistance, and philosophy of the program managers. There are currently active programs that use imaging because: it is mandatory to screen the general population<sup>2</sup>; smear microscopy and culture are unavailable; of the predominant number of smear-negative patients suspected of having TB<sup>1</sup>, HIV-infected patients require exclusion of active TB before initiation of highly active antiretroviral therapy (HAART); radiographs are useful to guide a change, continuation, or termination of treatment in patients with drug-resistant TB; only the tuberculin skin test is positive in a patient without symptoms; at the end of treatment it is useful to predict relapse of disease.<sup>9</sup> More advanced programs use: computed tomography (CT) when radiographs are normal or equivocal but there are symptoms of TB; multidetector CT with multiplanar reconstruction in an attempt to replace bronchoscopy in complicated lymphobronchial TB<sup>10</sup>; ultrasound to

diagnose TB lymphadenopathy in children; magnetic resonance imaging (MRI) to detect and differentiate TB lymphadenopathy from other causes of mediastinal widening; positron emission tomography (PET) to differentiate solitary nodules of TB (tuberculoma) from other causes such as malignancy.<sup>11</sup> Conversely, there is no or little use of radiography when services are unavailable, expensive, require referral elsewhere, are poorly performed or interpreted, or when other more specific tests are proving successful.

## DIFFERENCES IN IMAGING CHILDREN AND ADULTS

Children are different in size, anatomy, and physiology from adults. The thymus for example confounds interpretation of the mediastinal width on radiographs. Children are also imaged with a different technique to adults (anteroposterior (AP) instead of posteroanterior (PA) with different settings), provide opportunities for alternative imaging (imaging the mediastinum using ultrasound), and require significant considerations with regard to radiation dose.

## IMAGING FINDINGS

### *Lymph Node TB (Gangliopulmonary TB)*

TB lymph nodes in the mediastinum and hilar regions drain a primary parenchymal focus of

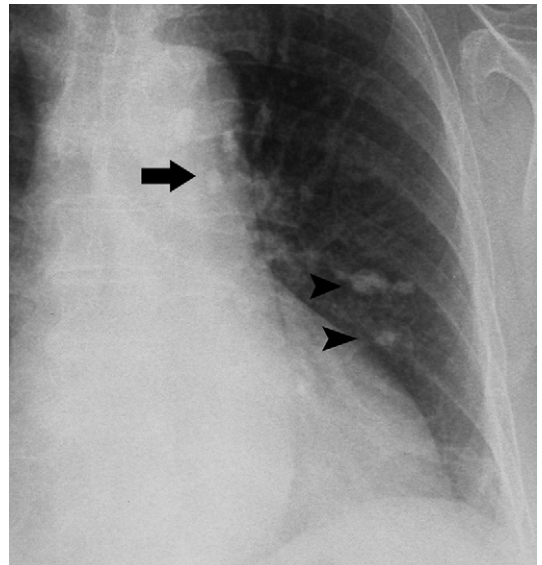


**Fig. 1.** Calcified Ghon (Ranke) complex. Plain radiograph (detailed view of the left hilum and left lower lobe). Note the presence of multiple calcified parenchymal foci in the lingula and calcified lymph nodes at the left hilum (arrowhead) and aortopulmonary window (black arrow).

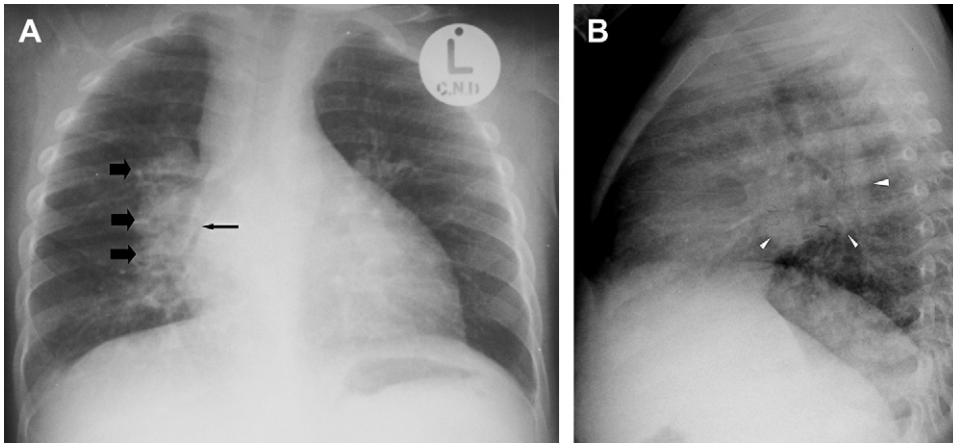


**Fig. 2.** Hilar lymphadenopathy (gangliopulmonary TB) in a child. (A) On the AP radiograph there is a multilobulated mass of lymph nodes projecting beyond the right cardiac margin (*short arrows*). There is resultant compression of the bronchus intermedius (*long arrow*). (B) On the lateral radiograph there is an oval dense mass often referred to as a “doughnut” representing a mass of hilar lymphadenopathy (*arrowheads*).

infection. Together the parenchymal focus and lymphadenopathy are known as the “Ghon complex” (**Fig. 1**).<sup>12</sup>

Lymphadenopathy was not a major feature of what was previously termed “postprimary TB” in adults (only 5% of cases),<sup>13</sup> but recently, especially with HIV coinfection, this tendency has reversed. Enlarged TB lymph nodes may cause complications involving the airways and other surrounding structures (see later discussion on complications of lymphobronchial TB).

### Chest radiographs (CXR)

Parenchymal abnormality may be small, peripheral, and difficult to identify.<sup>11</sup> In children and immune-suppressed adults, the focal abnormality may not be contained and may present as an air-space process (see later discussion on air-space disease).<sup>14,15</sup> Lymphadenopathy in children is only obvious when it projects beyond the cardiac margins and is less often seen on the left (**Fig. 2A**). Lateral radiographs are useful for detecting lymphadenopathy posterior and inferior to the bronchus intermedius (**Fig. 2B**). Calcification of lymphadenopathy (and the pulmonary focus) represents a healed lesion but is rare in childhood (**Fig. 3**).

### CT

Characteristic TB lymphadenopathy shows the “rim sign” on contrast-enhanced studies, with a low density center and an enhancing rim (**Fig. 4A, B**).<sup>16,17</sup> There are other causes for the rim sign including atypical mycobacteria,<sup>18</sup> lymphoma, and carcinoma.<sup>12</sup> More delicate and bizarre enhancement patterns particularly in matted nodes

in children have been described as ghostlike (**Fig. 5**).<sup>14</sup> Calcification is easily detected on CT particularly in adults but is rare in children (**Fig. 6**).<sup>14</sup>

### MRI

Lymphadenopathy may have a characteristic low signal on T2-weighted short Tau inversion recovery (STIR) imaging, probably related to free radicals, which are paramagnetic and associated with caseous necrosis (**Fig. 7A, B**). Some TB

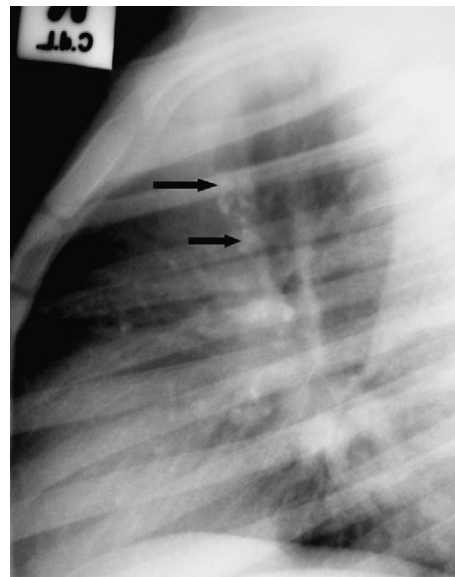


**Fig. 3.** Calcification on a lateral radiograph in a child. Small calcified foci (*arrows*) representing calcification within TB lymphadenopathy are an unusual finding in children.

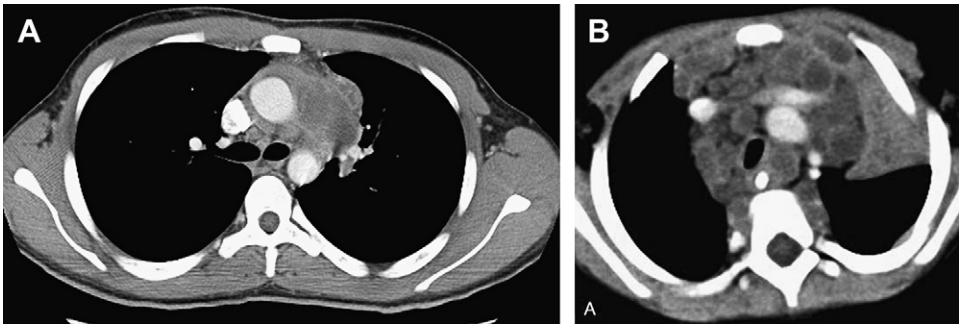


**Fig. 4.** Lymph node TB (gangliopulmonary tuberculosis). (A) Contrast-enhanced CT image at the level of the aortic arch in an adult showing huge lymph nodes with a necrotic center and peripheral rim enhancement. Note also some smaller solid enhancing lymph nodes anterior to the carina (*Courtesy of Dr. A. Snoeckx, Antwerp, Belgium*). (B) CT reveals multiple rim-enhancing TB lymph nodes in the mediastinum of a child, clearly demarcated from each other and from the thymus, which is displaced to the left. Note that the trachea is compressed from either side by lymphadenopathy. (*From Andronikou S, Wieselthaler N. Imaging for tuberculosis in children. In: Schaaf HS, Zumla A, editors. Tuberculosis: a comprehensive clinical reference. Philadelphia: Saunders Elsevier; 2009. p. 266; with permission.*)

lymphadenopathy shows solid nodular enhancement, whereas necrotic nodes show rim enhancement (**Fig. 8A, B**).

#### ***Air-space Parenchymal Disease (Consolidation)***

This pattern is seen with primary infection (especially in children) as a complication of bronchial erosion and resultant bronchogenic spread of disease or as a complication of bronchial compression with distal parenchymal disease including volume changes (collapse or hyperexpansion). During primary infection the small peripheral focus forms a granuloma, which limits initial replication and spread.<sup>15</sup> In children predominantly, the infection is not well controlled with increasing numbers of mycobacteria and dissemination via lymphatics and the blood stream. Air-space disease is seen in approximately 25% of children with TB.<sup>14</sup>

#### **CXR**

Confluent areas of opacity often affecting 1 lobe (**Fig. 9A**) and showing air bronchograms and a positive “silhouette sign” (obliterating the crisp cardiac, mediastinal, or diaphragmatic margins) (**Fig. 9B**) are the main features. The edge of an air-space process may be ill defined or may be well defined by a fissure that may bulge when there is volume gain (**Fig. 9C**). In children these may occur in any part of the lung parenchyma.

#### **CT**

Lung becomes isodense to muscle and shows air bronchograms. Viable (non-necrotic) lung tissue enhances with contrast and shows enhancing

vessels branching within it (**Fig. 10**), whereas necrosis shows lower density and does not enhance, often losing the vascular detail.

#### **MRI**

The signal of air-space disease is isointense to muscle on T1-weighted MR images and hyperintense on T2-weighted imaging (see **Fig. 7B**). The signal enhances with intravenous gadolinium when there is no necrosis (**Fig. 11**). The type of necrosis that may take place can be distinguished using T2-weighted imaging. Liquefactive necrosis



**Fig. 5.** CT in a child with primary infection shows characteristic ghost like enhancement. The lymph nodes have various shapes with a suggested translucency created by faintly enhancing margins and low density necrotic centers. (*From Andronikou S, Wieselthaler N. Imaging for tuberculosis in children. In: Schaaf HS, Zumla A, editors. Tuberculosis: a comprehensive clinical reference. Philadelphia: Saunders Elsevier; 2009. p. 266; with permission.*)

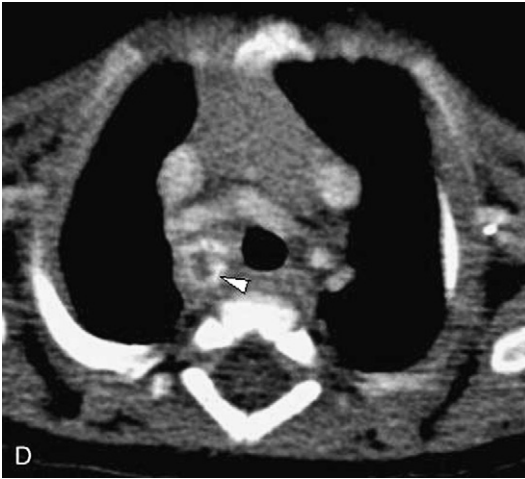


**Fig. 6.** CT image in a child shows calcification of right paratracheal lymphadenopathy (*arrowhead*) better than plain radiography. (From Andronikou S, Wiesenthaler N. Imaging for tuberculosis in children. In: Schaaf HS, Zumla A, editors. Tuberculosis: a comprehensive clinical reference. Philadelphia: Saunders Elsevier; 2009. p. 266; with permission.)

has a high T2 signal and caseous necrosis a low T2 signal within the lung, which already has a high T2 signal caused by the air-space process.

#### Tuberculoma/Parenchymal Nodules

Round or oval lesions involving the lung parenchyma in TB are usually granulomas. By definition,

granulomas greater than 1 cm are termed tuberculomas. Tuberculomas may show central necrosis and cavitate. Only calcified lesions should be considered inactive.

#### **CXR**

Lesions are round or oval and show smooth, sharply defined margins (**Fig. 12A**). Size varies from 0.4 to 5 cm and the majority are stable in size over time (**Fig. 12B, C**). Calcification is present in 20% to 30% of tuberculomas in adults. In 80% of tuberculomas there are characteristic satellite lesions in the immediate vicinity of the main lesion (see **Fig. 12B, C**).

#### **CT**

Lesions are more easily identified (**Fig. 13**) and CT is more sensitive for showing calcification. Some lesions may show central low density in keeping with necrosis.

#### **MRI**

Tuberculomas are isointense to muscle on T1-weighted images but on T2-weighted images signal intensity varies according to the stage/type of necrosis (liquefactive necrosis being of high signal and caseous necrosis of low signal intensity (**Fig. 14**)).

#### Miliary Pattern

Miliary nodules result from and indicate haematogenous dissemination of TB bacilli into the lungs and other organs, where innumerable

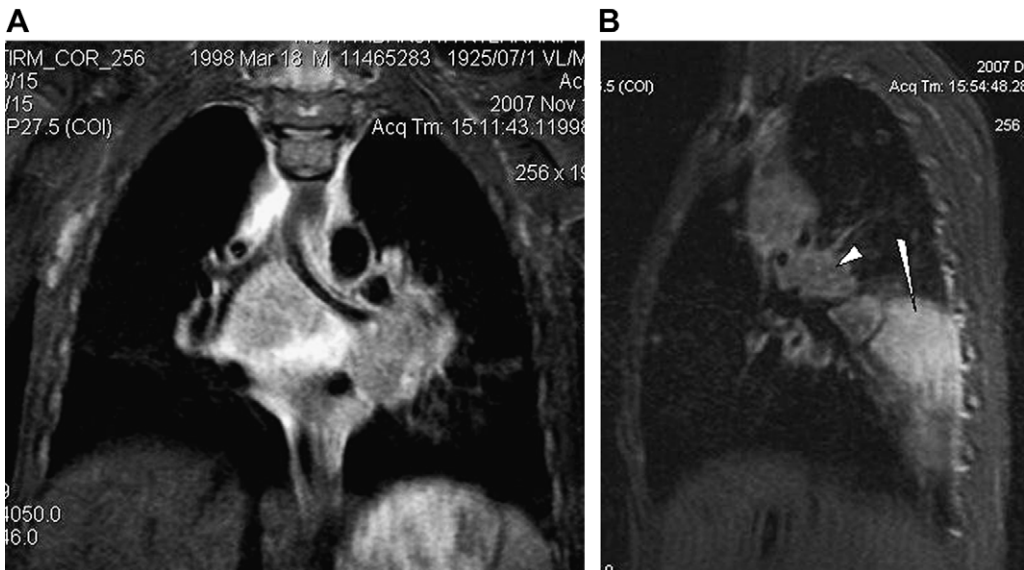


**Fig. 7.** (A) Coronal and (B) sagittal STIR MRI images show a characteristic low signal to subcarinal and hilar lymphadenopathy that is believed to result from free radicals. Note how the low signal of the lymphadenopathy (*short arrowhead*) contrasts with the high signal of the consolidated lung (*long arrowhead*) in (B).

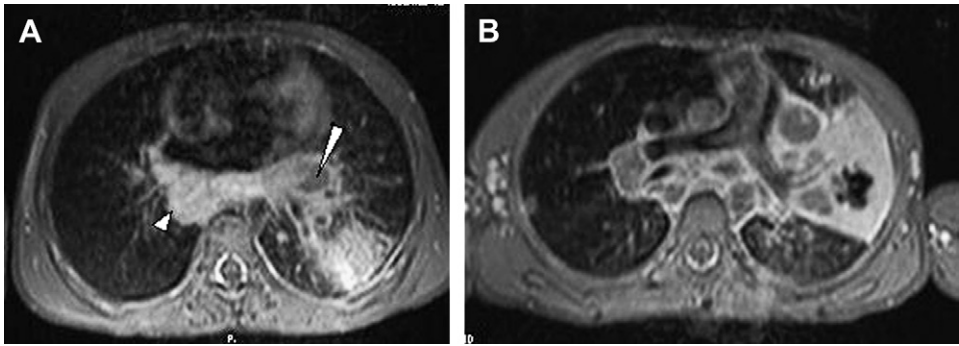


**Fig. 8.** Axial gadolinium-enhanced MRI reveals nodular (*short arrowhead*) and rim-enhancing (*long arrowhead*) lymphadenopathy in (A), and distinctly rim-enhancing lymphadenopathy in (B). Note also the enhancing lung parenchyma where there is air-space disease and an area of signal void where there is an air-filled cavity.

granulomas develop. This is classically seen in children in endemic areas (up to one-third of cases)<sup>14</sup> but there is an increasing incidence in adults.

#### **CXR, CT, MRI**

Innumerable nodules of similar size (1–4 mm) are scattered randomly and diffusely throughout both lungs (**Fig. 15A**). By definition the nodules, being

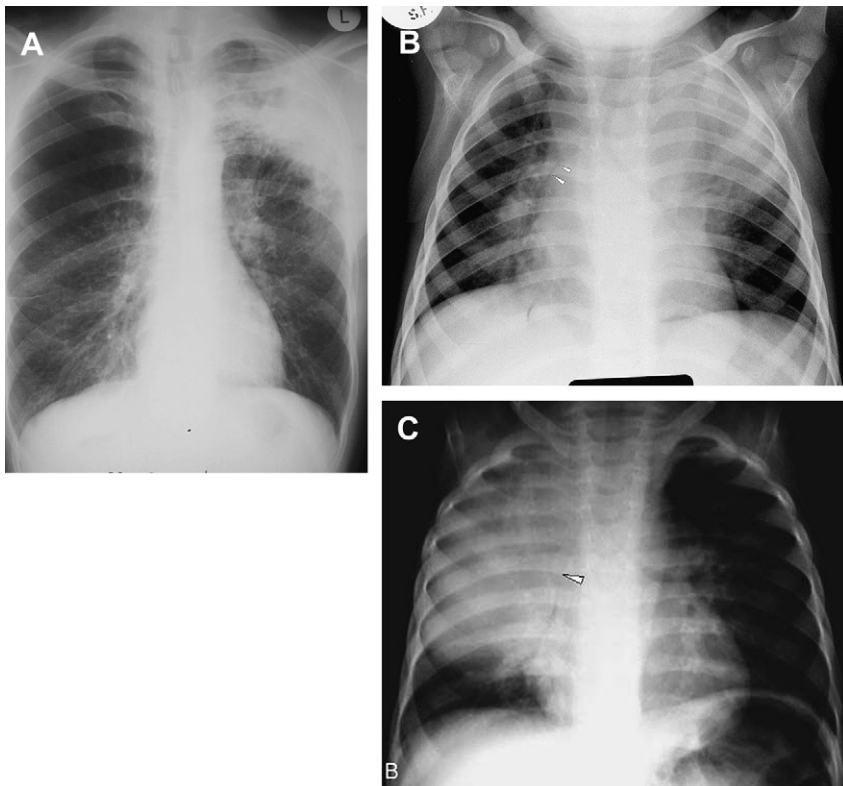


**Fig. 9.** Air-space disease. (A) Plain radiograph shows a confluent area of peripheral density in the left upper lobe of an adult with primary infection. (*Courtesy of Steve Beningfield, University of Cape Town, South Africa*). (B) Typical primary infection in a child showing left upper lobe confluent density of an air-space process. In addition there is right hilar lymphadenopathy causing compression of the bronchus intermedius (*arrows*). (C) The right-sided air-space process in this child has a bulging inferior margin in keeping with an exudative process. In this case it is caused by compression of the right main bronchus by tuberculous lymphadenopathy (*arrow*). (*From Andronikou S, Wieselthaler N. Imaging for tuberculosis in children. In: Schaaf HS, Zumla A, editors. Tuberculosis: a comprehensive clinical reference. Philadelphia: Saunders Elsevier; 2009. p. 268; with permission.*)

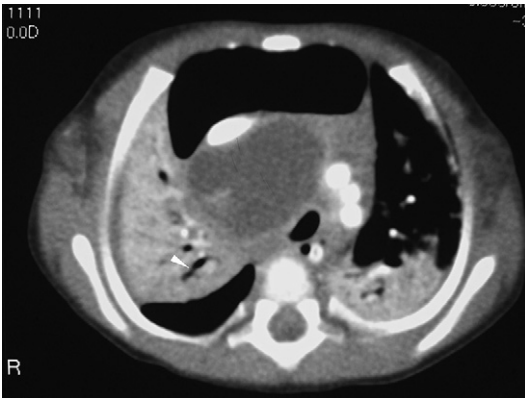


**Fig. 10.** Air-space disease in a child with primary infection. CT scan shows the imaging characteristics of air-space disease on the right (and less prominent on the left). There is confluent density, which is enhancing, indicating that the lung is viable. There are air bronchograms (*arrowhead*) and visible enhancing vessels. There is also a large necrotic right paratracheal lymph node compressing and displacing the distal trachea.

interstitial, do not coalesce and remain discretely margined (**Fig. 15B**). Even though the appearance is easily recognized on CXR, high-resolution CT (HRCT) is ideally suited to showing these and often also shows interlobular septal thickening (**Fig. 15C**).<sup>14,19</sup> A tip for distinguishing nodules from normal vessels for inexperienced observers is to look in the costophrenic angles and the peripheral 1 cm of the lungs where few vessels are expected.

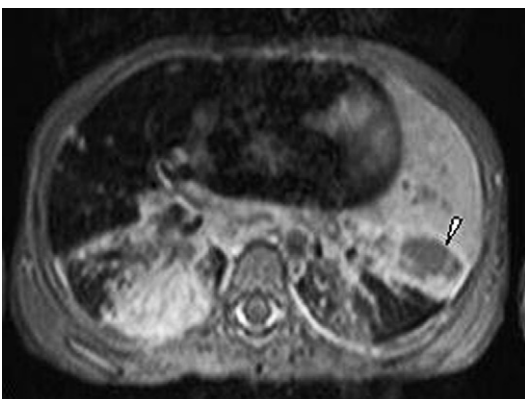


**Fig. 11.** Air-space disease in a child. MRI scan with intravenous gadolinium contrast shows enhancement (and therefore high signal) involving the dependent portion of the right lung where there is an air-space process. A large confluent area in the left lung is not as brightly enhancing (indicating early necrosis) and shows an oval area where there is low signal in keeping with advanced necrosis (*arrowhead*).

## Cavities

These are formed by liquefaction of caseous necrosis and subsequent fibrosis with lung destruction. They are reported to occur in 40% to 50% of adults with a new diagnosis of TB. They also occur in children and should not be considered as an indication of reinfection. Risk of relapse after anti-TB treatment is significantly higher in patients with cavities whether these are present early on during treatment or at the end of treatment.<sup>9</sup> It is also important to recognize cavities and report their position for surgical management when treatment options become limited. There are 4 mechanisms described for cavity formation:

- primary cavitation as early as 6 months after primary infection (**Fig. 16A**)
- reactivation of previous hematogenous spread with confluence of nodular lesions
- bronchial cavities caused by bronchiectasis or bronchial perforation and distal parenchymal cavitation
- Exogenous reinfection<sup>4,6,7</sup>

## CXR and CT

Air-filled oval areas within an opacity (**Fig. 16B**) or a nodule (**Fig. 16C**) represent cavitation. “True” cavities have thick walls (3 mm) and may be nodular or smooth, whereas bullae or pneumato-coeles have thin walls and little surrounding opacity (**Fig. 16D**). Air-fluid levels occur within 10% of cavities (**Fig. 16E**) (often caused by superinfection). Bronchiectasis is more difficult to confirm on CXR by identification of “ring shadows” with thick walls and parallel tubular markings (“tram-track sign”). HRCT shows the characteristic “signet-ring sign” of the ectatic thick-walled bronchus (representing the ring portion) adjacent to the smaller blood vessel (representing the “gem” of the ring). Traction bronchiectasis exists within distorted lung parenchyma with elevated fissures or hila and pleural adhesions (**Fig. 16F**).<sup>12</sup>

## Pleural TB

Previously, exudative pleuritis was seen mainly in older children and adolescents. It is currently also seen in adults (in countries with a low incidence of TB infection) and younger children. It occurs 3 to 6 months after primary infection and is often unilateral (and asymptomatic). Pleural fluid only yields culture of the organism in 20% to 40% of samples in patients with TB.<sup>20</sup>

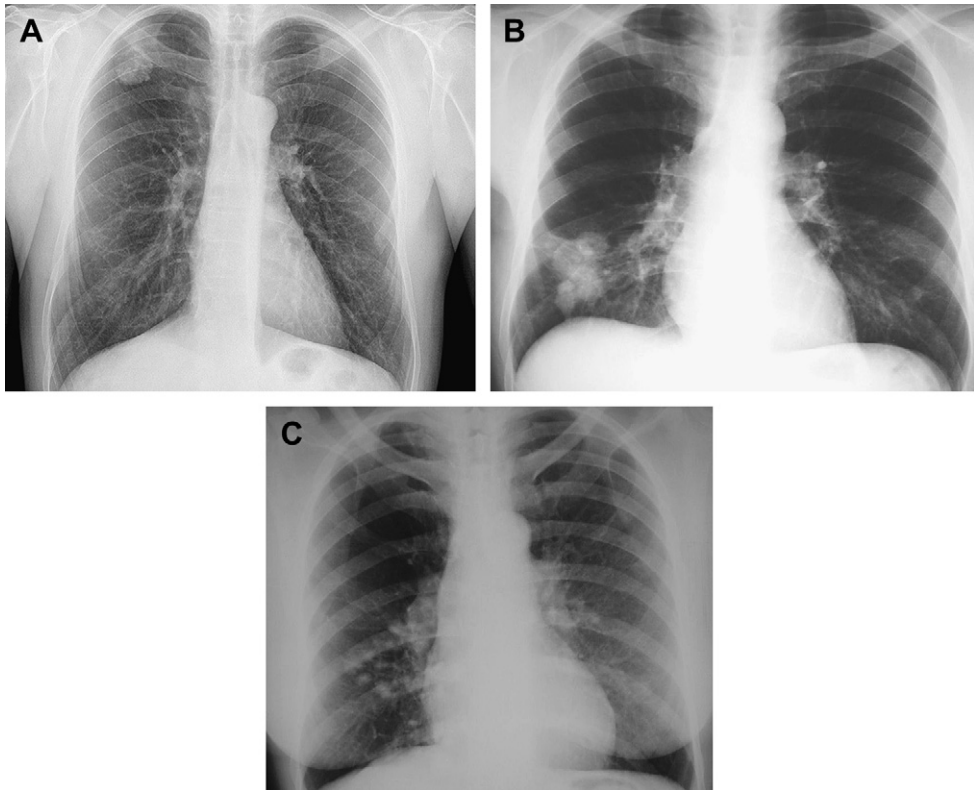


**Fig. 12.** Tuberculoma. (A) A large partially calcified tuberculoma is present in the right upper lobe on a plain radiograph. (B) The large tuberculoma in the right lower zone seems to represent a conglomerate predominant lesion with some satellite foci. (C) A group of tuberculous parenchymal granulomata in the right lower zone of an adult female. (Images (B) and (C) courtesy of Steve Beningfield, University of Cape Town, South Africa).

### CXR

Effusions are usually accompanied by parenchymal and nodal disease.<sup>17</sup> They may, however, be the only radiographic sign in a minority of primary TB infections. Blunting of the costophrenic angle alone in adults is not considered significant for active disease by the Centers for Disease Control and Prevention (CDC) as a CXR screening criterion. Only larger amounts of pleural fluid are taken into consideration.<sup>21</sup> Pleural apical capping is also not considered to be suggestive of active TB disease and may represent fatty proliferation (Fig. 17).<sup>21</sup>

### Ultrasound

Ultrasound (US) is a useful and rapid way of detecting pleural fluid and guiding a pleural tap.

### CT

Contrast-enhanced scans show thickening of the visceral and parietal pleura (“split-pleura sign”).<sup>22</sup>

### Fibrosis, Scarring or Destruction

Complete or partial destruction of the lung is not uncommon in the end stage of parenchymal and

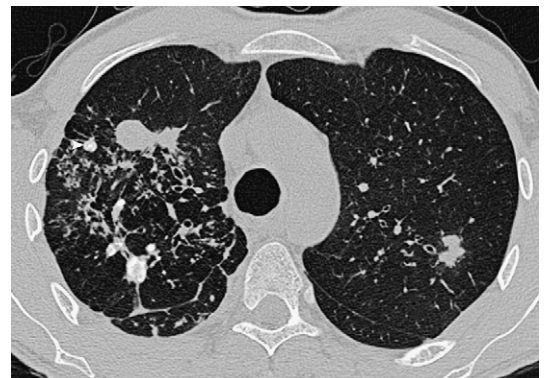


**Fig. 13.** Tuberculomata. Axial CT scan showing multiple tuberculous granulomas of variable size within the upper lobes. Note central calcification in 1 lesion (white arrowhead) and associated thickening of the bronchial walls, thickening of the fissures, and “tree-in-bud” pattern.

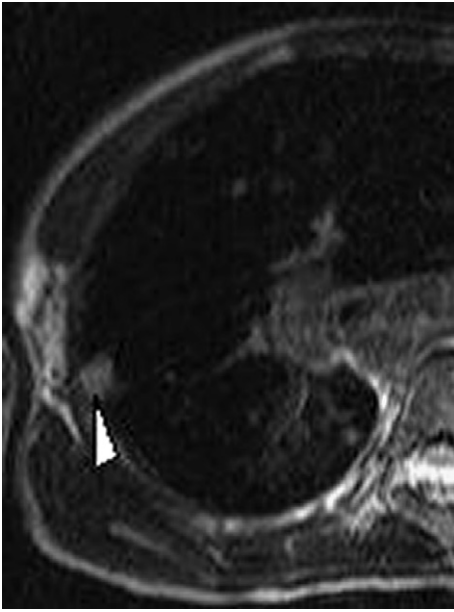


**Fig. 14.** Tuberculoma. MRI (STIR sequence) shows a peripheral tuberculoma in the right lung (*arrow-head*) with characteristic low signal intensity in keeping with caseous necrosis.

airway involvement. Fibrosis may be stable, progress or regress, but once the lung is destroyed, activity is difficult to assess.

#### **CXR/CT**

Cicatrization atelectasis is common after cavitory disease and involves atelectasis of the upper lobe, retraction of the hilum, compensatory hyperinflation of the lower lobe, and mediastinal shift toward the fibrotic lung.<sup>12</sup> Distortion of lung parenchyma with volume loss also results in pleural adhesions (**Fig. 18**) and formation of traction bronchiectasis. Apical pleural thickening is another association of fibrosis and may be caused by proliferation of extrapleural fat and peripheral atelectasis.<sup>12</sup>

#### **IMPORTANT ADDITIONAL CONSIDERATIONS**

##### ***Drug Resistance (Multidrug-Resistant or Extensive Drug-Resistant TB)***

Multidrug-resistant (MDR) TB is resistance to isoniazid and rifampicin. Extensive drug-resistant (XDR) TB is MDR plus resistance to the fluoroquinolones and at least 1 of the second-line injectable

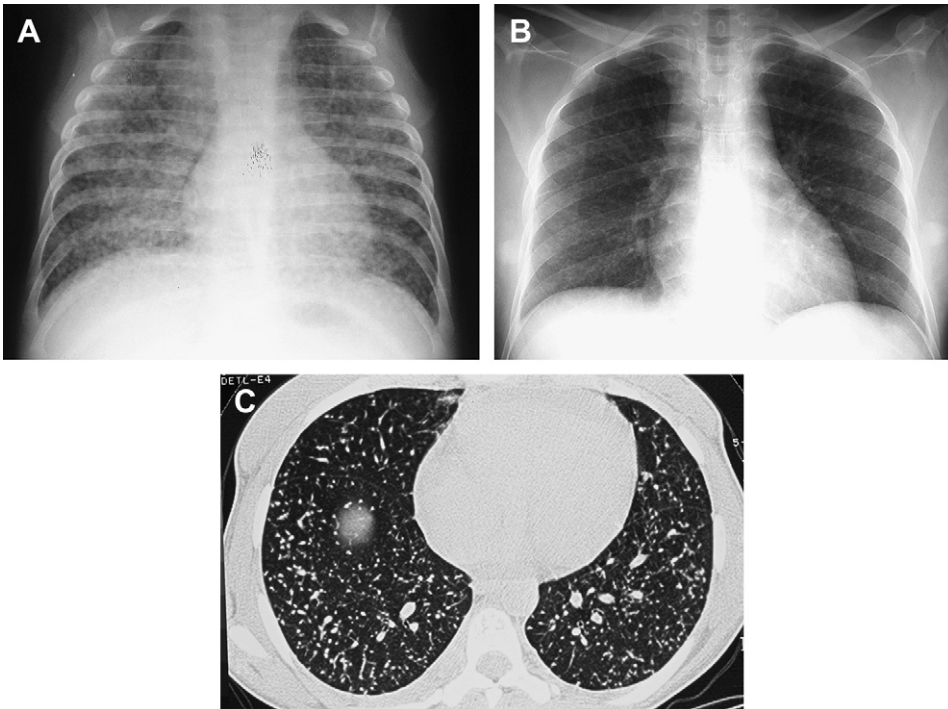


**Fig. 15.** Miliary tuberculosis. (A, B) Plain chest radiographs showing diffuse 2- to 3-mm widespread nodules throughout the lungs. (From Andronikou S, Wieselthaler N. Modern imaging of tuberculosis in children: thoracic, central nervous system and abdominal tuberculosis. *Pediatr Radiol* 2004;34(11):85; with kind permission of Springer Science + Business Media.) (C) High-resolution CT showing multiple small nodules in a random distribution. Note subtle subpleural and subfissural nodules.

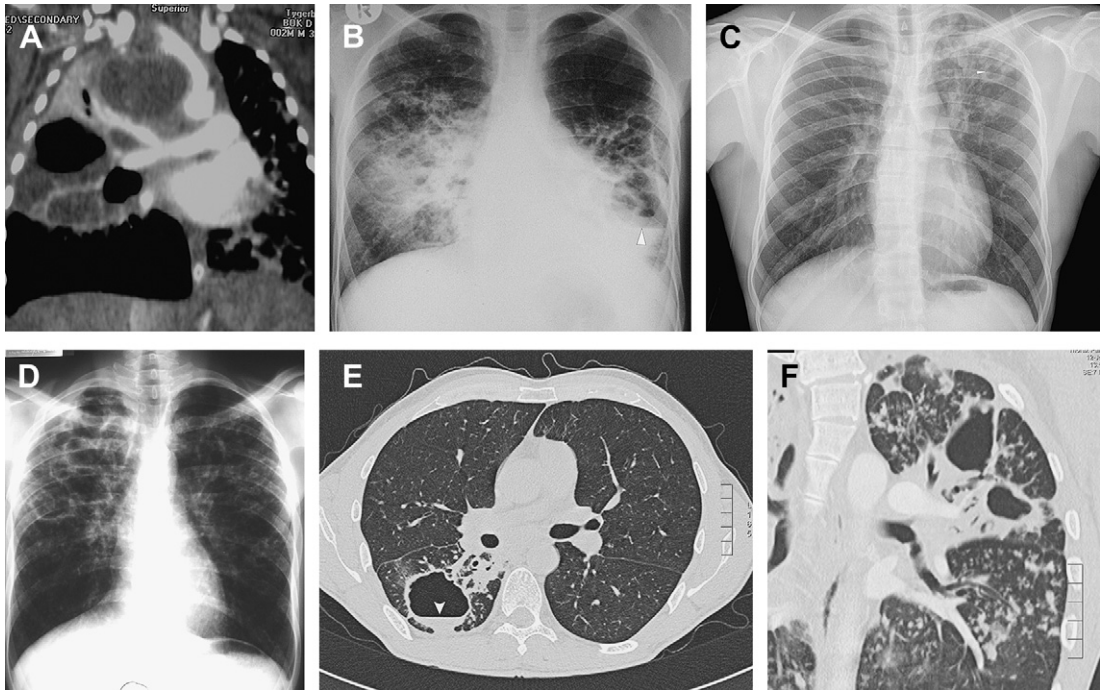


**Fig. 16.** Cavities. (A) Coronal reformatted CT in a child with primary infection showing multiple cavities in the right lung and necrotic mediastinal lymphadenopathy. (B) Plain radiograph in an adult showing multiple cavities developing bilaterally within large areas of air-space disease. There are air-fluid levels within some of the cavities (*arrowhead*). (C) Plain radiograph of a thick-walled cavity that has developed within an apical tuberculoma (*arrow*). (D) Multiple thin-walled cavities within the right upper zone. (E) CT image showing an air-fluid level (*arrowhead*) in a cavity within the apex of the right lower lobe. (F) Cavities occurring in association with lung distortion and associated endobronchial TB shown on coronal CT scan. There are multiple thick-walled cavities within the left upper lobe, ill defined apicohilar opacities, extensive distortion of the lung parenchyma and hila, and thickening of the apical pleura. Note also traction bronchiectasis and endobronchial spread (“tree-in-bud” sign).

drugs. Imaging plays a role in identifying lesions contributing to drug resistance such as large cavities, which harbor mycobacteria within an area where there is limited drug penetration.

#### **CXR and CT**

Two imaging patterns have emerged. Patients with new drug resistance (ie, no previous TB treatment or treatment for  $\leq 1$  month) usually show noncavitating disease and pleural effusion. Patients with MDR and a history of previous anti-TB treatment longer than 1 month show cavitating disease. Overall, patients with drug-resistant TB show multiple cavities and bronchiectasis more commonly (**Fig. 19A, B**).<sup>17</sup> Identification and localization of cavities on CT serves as a road map for planning surgery.<sup>17</sup>

#### **AIDS, HIV Coinfection and Immune Reconstitution Inflammatory Syndrome**

HIV infection enhances the susceptibility to TB, hastens its progression, and makes it more likely for a patient to be exposed to a case of TB.<sup>15</sup>

Patients infected with HIV can have massive hematogenous dissemination after initial infection, resulting in a higher risk for a fulminant course. TB is a major cause of death in patients with HIV. CXR for TB in patients with HIV may be confusing



**Fig. 17.** Pleural calcifications in an elderly patient with a past history of tuberculous pleuritis. Plain radiograph shows extensive calcification of the pleura.



**Fig. 18.** Fibrosis and scarring. There are long linear densities in the left upper zone with distortion of lung architecture, in addition to multiple cavities. The right and left hila are displaced superiorly by traction from the fibrotic scarring.

because TB and HIV share some imaging features, TB features may be more severe in patients with HIV, there are multiple possible pathologic conditions that may occur simultaneously (Kaposi

sarcoma, lymphocytic interstitial pneumonitis, bacterial pneumonia), and because CXR in patients with TB and HIV coinfection may be normal.<sup>15</sup>

#### **CXR and CT**

Appearances depend on the level of immunosuppression.<sup>23</sup>

- Early stage (immunocompetent) CD4 200–500/mm<sup>3</sup>: appearances are those of postprimary disease<sup>24</sup>
- Late stage (immunosuppression) CD4 <200/mm<sup>3</sup>: up to 20% of CXR may be normal<sup>12,25</sup>; findings are usually those of lymph node TB regardless of previous exposure<sup>24,26</sup>
- Severe and advanced (immunosuppression) CD4 <100/mm<sup>3</sup>: nonspecific findings with diffuse coarse pattern<sup>24</sup>
- All stages and degrees of immunosuppression: miliary<sup>23,27</sup>
- Post-HAART initiation (restored immunity): development of immune reconstitution inflammatory syndrome (IRIS) represents a paradoxical clinical and radiological reaction to antigens from TB infection that provokes an inflammatory response. Worsening or new lymphadenopathy, pulmonary disease, and/or effusion are the major chest features.<sup>28</sup>

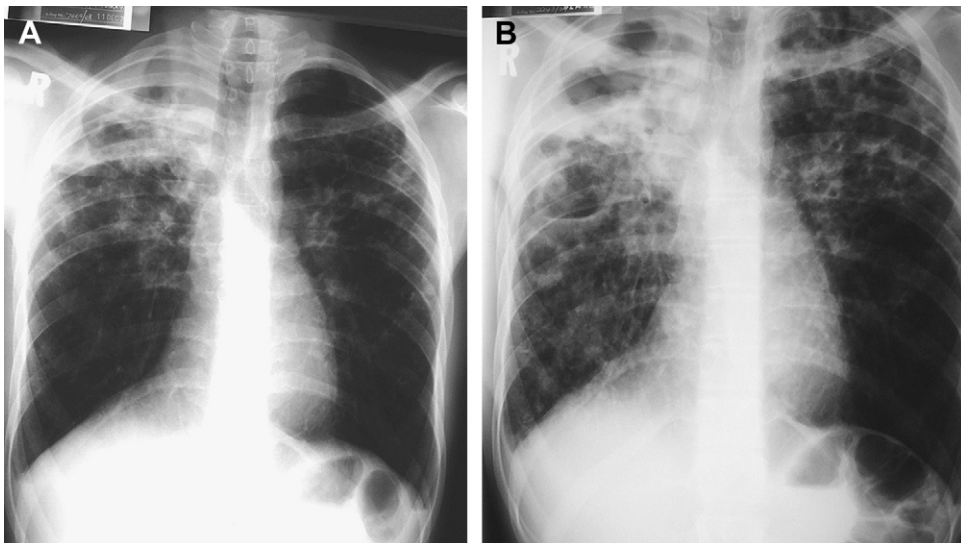


**Fig. 19.** Multidrug-resistant (MDR) TB with (A) initial, and (B) 5-month follow-up radiographs. (A) The initial radiograph shows that in addition to the bilateral upper zone ring shadows representing traction bronchiectasis and thin-walled cavities, there is a confluent process in the right upper zone containing thick-walled cavities suggestive of active disease. The active cavitating disease indicates a higher risk for relapse of disease. (B) The routine follow-up radiograph (for management decisions in MDR TB) at 5 months shows that the right upper zone process has extended rather than resolved, with further cavitation and fluid levels in the right mid-zone. There was no culture conversion of sputum in this patient requiring revision of therapy and further drug susceptibility testing.

### ***Infection Versus Disease, Active Versus Inactive Disease***

Distinguishing TB infection from disease is important as treatment differs (from 1 drug to 3–4 drugs) and because laboratory tests are often unable to make this distinction. This is difficult in children because of the rapid progression from infection to disease. Parenchymal air-space or miliary patterns, lymphadenopathy, and pleural effusion are considered to represent disease. A single non-cavitating, calcified granuloma (Ghon focus) is considered to represent previous infection.

The distinction between active and inactive disease has numerous implications including therapeutic and social (immigration, employment, and health care benefit). Once the lung is destroyed, activity is difficult to assess with radiology studies because fibrosis is known to regress or remain stable. Air-space disease and cavities, with or without lymphadenopathy, are considered active disease. High-resolution CT shows large nodules, “tree-in-bud” densities, lobular consolidation, or mass lesions, and is considered the most accurate imaging method for determining activity.<sup>29</sup> Nodules and scars may contain slowly multiplying TB bacilli and have the potential to progress to active disease.<sup>21</sup> Patients infected with HIV are a greater challenge as even a normal CXR may be associated with active disease.<sup>21</sup> Labeling CXR features as inactive TB should be done with caution. Pulmonary nodules without fibrotic scars and volume loss are considered to represent old healed TB, but it is better to only consider these findings as inactive when smear or culture is negative and the CXR findings are stable over time.<sup>12</sup> Calcified nodular lesions have a low risk of active disease.<sup>21</sup>

### **COMPLICATIONS**

#### ***Progressive Primary TB***

Children with progressive primary disease tend to have extensive cavitations and are very ill. They often require admission and ventilation. There is a high mortality rate.

#### ***CXR and CT***

Multiple cavities are seen throughout both lungs with surrounding air-space disease (Fig. 20).<sup>30</sup>

#### ***Lymphobronchial TB***

Lymph node TB may be complicated by perforation of adenopathy into a bronchus with obstructive pneumonia/atelectasis (epituberculosis).

#### **CXR**

The lung parenchyma may show air-space disease (consolidation) or obstructive



**Fig. 20.** Progressive primary TB. Axial CT scan shows extensive bilateral air-space disease and multiple cavities in this young child who required ventilation and subsequently died. (From Griffith-Richards SB, Goussard P, Andronikou S, et al. Cavitating pulmonary tuberculosis in children: correlating radiology with pathogenesis. *Pediatr Radiol* 2007;37(8):802; with kind permission of Springer Science + Business Media.)

hyperinflation.<sup>19</sup> This usually affects the right main bronchus or bronchus intermedius (Fig. 9).<sup>12,31,32</sup>

#### **CT**

A progression from postobstructive air-space disease to bronchial filling by fluid (wet lung), progressive necrosis with loss of vascular markings, lack of lung parenchymal enhancement, bulging fissures, and eventual cavitation is well shown (Fig. 21).<sup>30,33</sup>

#### **MRI**

Lung necrosis shows nonenhancement within an area of consolidated enhancing lung parenchyma and a range of signal intensity possibilities on T2-weighted imaging. Caseous necrosis is of low signal intensity on T2-weighted images, whereas liquefactive necrosis, which is a precursor to cavitation, is of high signal intensity, and eventual cavitation with air shows signal void (Fig. 22).

#### ***Bronchogenic Spread and Tracheobronchial TB***

Bronchogenic spread complicates 2% to 4% of pulmonary TB disease.<sup>34</sup> This originates when there is perforation of lymphadenopathy into a bronchus.

#### **CXR**

Usually the radiograph is normal but parenchymal opacities, seen as ill defined micronodules that tend to coalesce in some parts, are noted

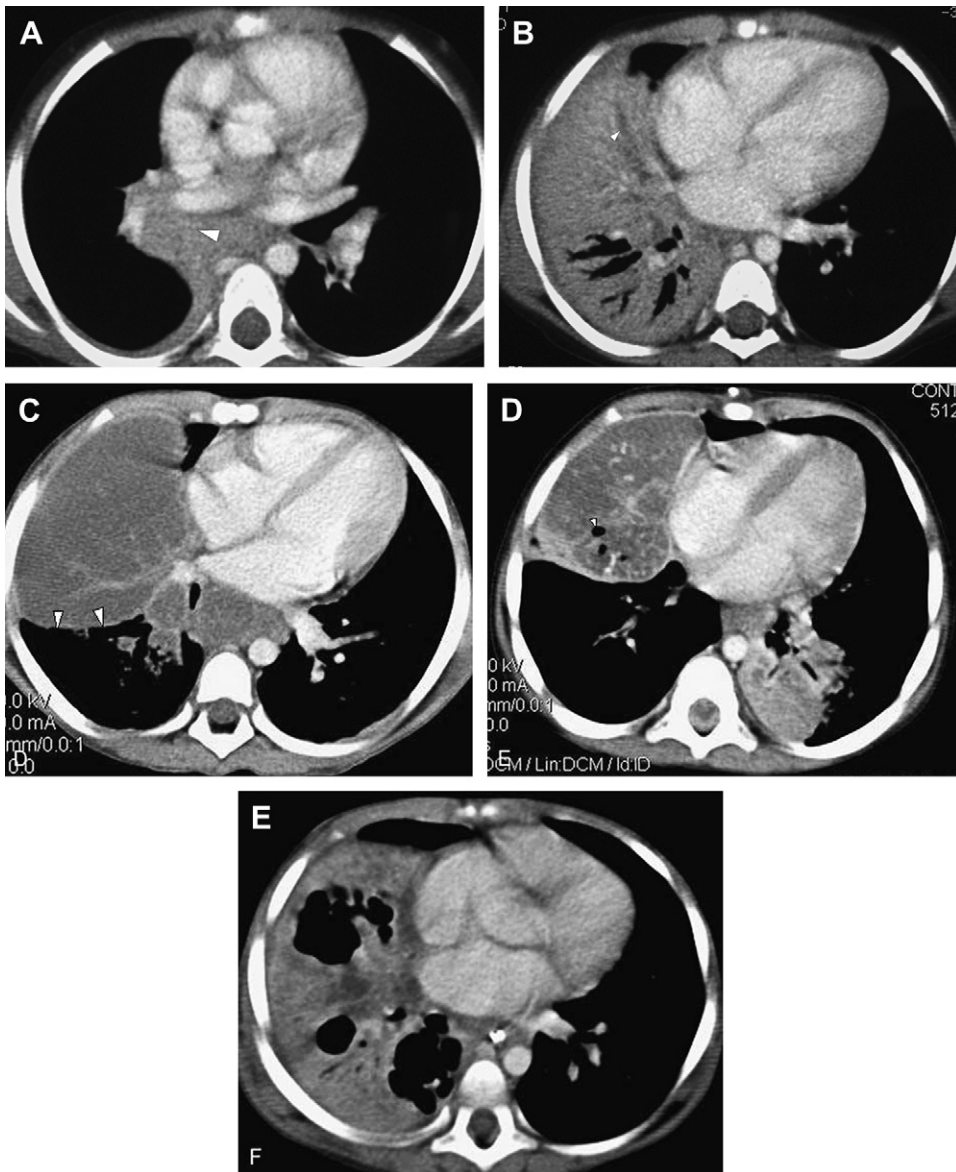


**Fig. 21.** Lymphobronchial TB. Progressive stages of the effects on the lung shown on contrast-enhanced CT (in different patients) from earliest (A) to latest (E). (A) Lymphadenopathy is seen involving the right hilum (*arrowhead*) and, unlike on the left, the right bronchus is not visible (it is compressed). (B) Distal to a right-sided compression, there is air-space disease. Posteriorly in the parenchyma there are air bronchograms and visible vessels. Anteriorly (the right middle lobe) the bronchi are filled with fluid (wet lung) (*arrowhead*). The lung enhances throughout. (C) Distal to the bronchus intermedius compression (by hilar and subcarinal lymphadenopathy) the right middle lobe shows nonenhancement, lack of visible bronchi, and a bulging margin (*arrowheads*) indicating a necrotic lung lobe that is expansile. (D) The right middle lobe necrosis shows early breakdown with air pockets (*arrowhead*). In contrast, the left lower lobe shows air-space disease with air bronchograms and enhancing parenchyma (in keeping with viability). (E) Advanced cavitation (air-filled areas) in multiple locations within the right lung, which also shows some areas of necrosis (low density, nonenhancing) and some areas of viable consolidated lung (enhancing with air bronchograms). (Parts (C), (D) and (E) from Andronikou S, Wiesenthaler N. Imaging for tuberculosis in children. In: Schaaf HS, Zumla A, editors. Tuberculosis: a comprehensive clinical reference. Philadelphia: Saunders Elsevier; 2009. p. 270; with permission.)

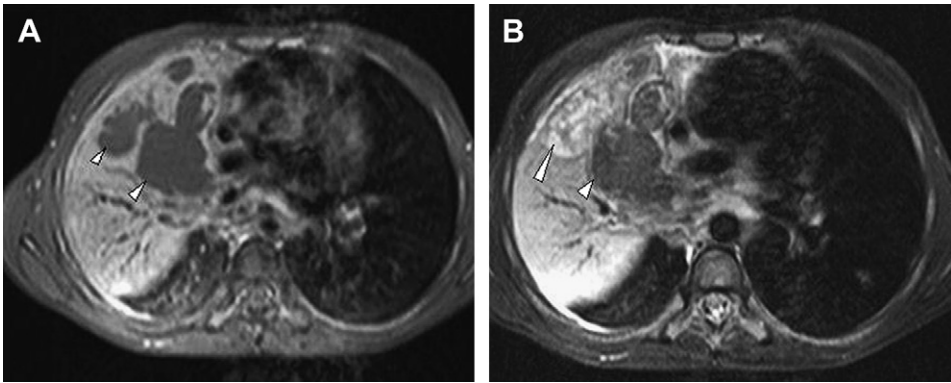


**Fig. 22.** MRI of lung necrosis. (A) Postgadolinium T1-weighted MR image shows right-sided necrosis as geographic areas of nonenhancing low signal (*arrowheads*) compared with the enhancing "solid" air-space disease containing air bronchograms. (B) STIR/T2 imaging shows that some areas of necrosis have characteristic low signal (caseous necrosis) (*short arrowhead*), whereas other areas show very high signal (liquefactive necrosis) (*long arrowhead*) easily distinguished from air-space disease, which is generally of high signal with air bronchograms.

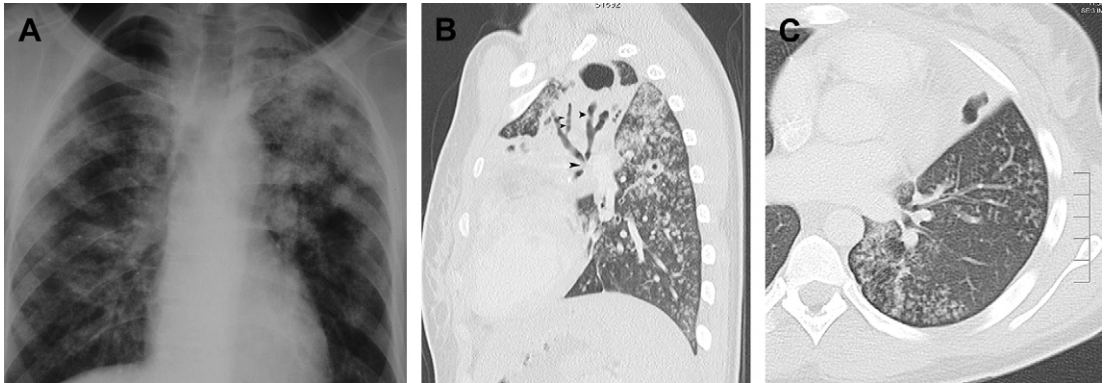


**Fig. 23.** Bronchogenic spread and tracheobronchial TB. (A) Plain radiograph shows widespread, fluffy nodules of various sizes with ill defined edges tending to confluence into areas of air-space disease (*left upper zone*) representing bronchogenic spread of TB. (B) Sagittal reformatted CT of the left lung showing multiple stenoses along the course of the left upper bronchi (*arrowheads*), thickening of the bronchial wall, ill defined opacity within the upper lobe, and linear branching opacities within the lower lobe ("tree-in-bud" pattern). Note associated cavitation in the apicoposterior segment of the left upper lobe. (C) Axial image in the same patient as in (B) showing "tree-in-bud" pattern in the left lower lung.

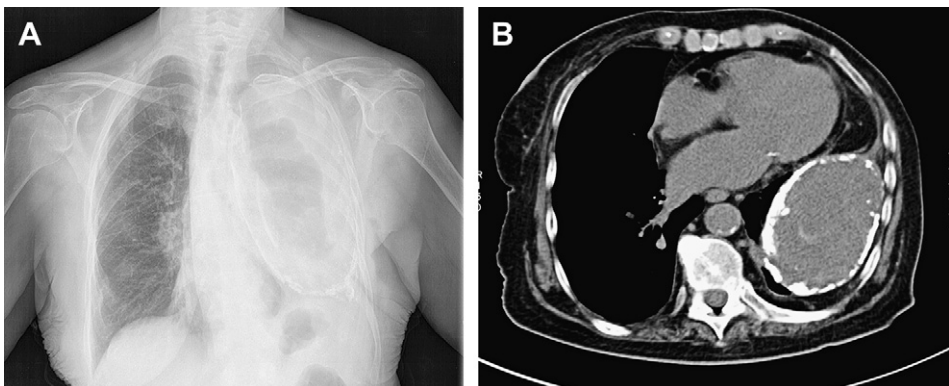


**Fig. 24.** Extensive pleural calcifications. (A) Plain radiographs and (B) CT showing extensive pleural calcifications on the left side.

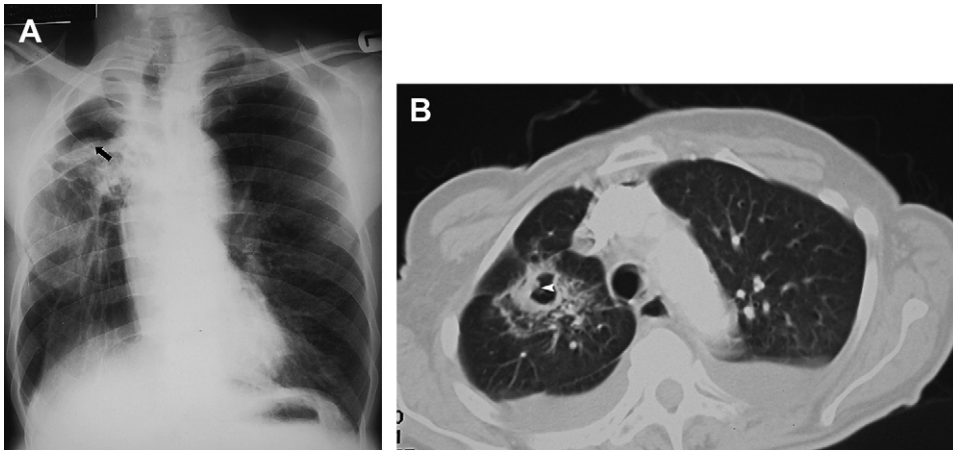


**Fig. 25.** Aspergilloma. (A) Plain radiograph shows a crescent lucency outlining an aspergilloma lying within a right upper zone cavity. Note the elevation of the right hilum caused by apical scarring on the right compared with the left. (B) Small aspergilloma (arrowhead) in a thick-walled cavitation in the right upper lobe. Note associated pleural effusion bilaterally.

(**Fig. 23A**). This is distinguished from miliary nodules, which have sharp edges and are discreet (ie, separable from each other).

#### HRCT

Acute tracheobronchial TB is seen as circumferential bronchial narrowing with mural thickening.<sup>35,36</sup> In the late phase the effects on the bronchus are cicatricial bronchiectasis (**Fig. 23B**).<sup>36</sup> Bronchogenic spread of TB is seen earlier and more often on HRCT than plain radiographs and presents as nodular and sharply branching opacities (“tree-in-bud” sign) (**Fig. 23C**).<sup>37</sup>

#### **Empyema, Bronchopleural Fistula, and Fibrothorax**

TB pleurisy may become localized causing an empyema. This can also break through the parietal

pleura to form a subcutaneous abscess<sup>38</sup> or communicate with the bronchial tree as a bronchopleural fistula.

#### CXR and CT

Empyema is shown as a focal fluid collection with pleural thickening (with or without calcification) (**Fig. 24**). Fibrothorax is shown as diffuse pleural thickening without pleural effusion and suggests inactivity.<sup>36</sup> Bronchopleural fistula shows air in the pleural space that has a changing air-fluid level on sequential CXR. On CT a direct communication may be seen between the pleural space and bronchial tree or lung parenchyma.<sup>39</sup>

#### **Aspergilloma**

A residual TB cavity can be colonized by *Aspergillus* and presents as an aspergilloma with

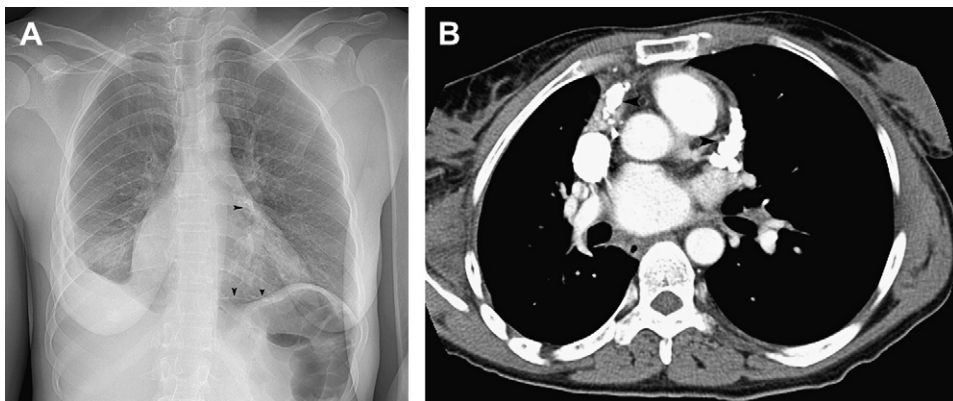


**Fig. 26.** Tuberculous pleuritis and sequelae of tuberculous pericarditis. (A) Plain radiograph showing right pleural effusion and coarse calcification of the pericardium (arrowheads). (B) Contrast-enhanced CT confirms thickening and coarse calcification of the pericardium (arrowheads). (Courtesy of Dr. A. Snoeckx, Antwerp, Belgium.)

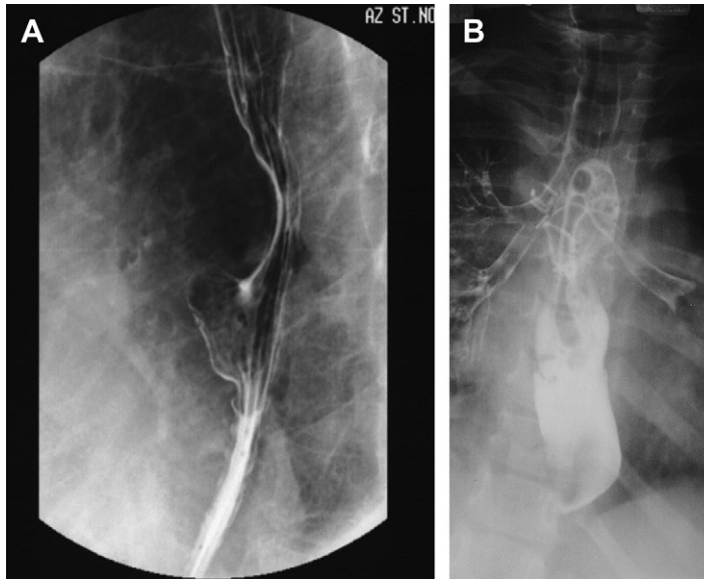


**Fig. 27.** Esophageal TB and trachea-esophageal fistula. (A) Traction diverticulae of the esophagus on a barium study, as a result of longstanding TB. (B) Contrast swallow in a child shows contrast entering the trachea and main bronchi in the absence of aspiration indicating a trachea-esophageal fistula. This was repaired using an esophageal stent.

hemoptysis in 60% of cases (and results in death in 5%).

#### **CXR and CT**

Early on there is thickening of the walls of a TB cavity and later a spherical nodule is seen with a crescent area of air separating the nodule from the adjacent cavity wall (**Fig. 25**).<sup>40</sup> The nodule is mobile on supine or prone positioning.

#### **TB Pericarditis and Pericardial Effusion**

TB pericarditis complicates 1% of TB cases and especially affects immunosuppressed individuals. In sub-Saharan Africa TB is the most common cause of pericardial effusion in adults<sup>41</sup> and effusion is seen in 14% of all TB cases (as high as 22% in those coinfecting with HIV).<sup>42</sup> In children with TB, pericardial effusion may be the result of severe malnutrition.<sup>41</sup> Constrictive pericarditis is a late complication affecting 10% of patients with TB pericarditis.<sup>36</sup>

#### **Ultrasound and CT**

Pericardial thickening with or without effusion are evident. There may be associated distension of the inferior vena cava, pleural effusions, and deformation of the interventricular septum.<sup>43</sup> Constrictive pericarditis is shown as thickening of the pericardium greater than 3 mm with or without calcification (**Fig. 26**).

#### **Myocardial TB**

This is a rare complication of TB usually associated with other foci of TB.

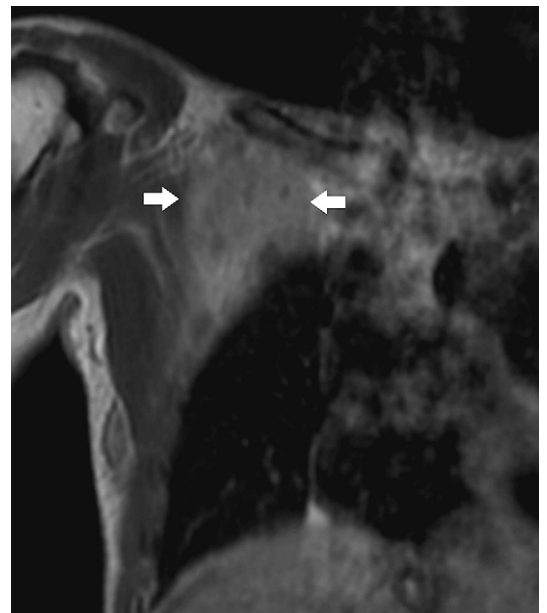


**Fig. 28.** Chest wall tuberculosis. Coronal fat-suppressed T1-weighted image after gadolinium contrast showing marked enhancement of a large soft tissue lesion at the right thoracic wall. The areas of central nonenhancement reflect caseation and/or liquefaction necrosis.

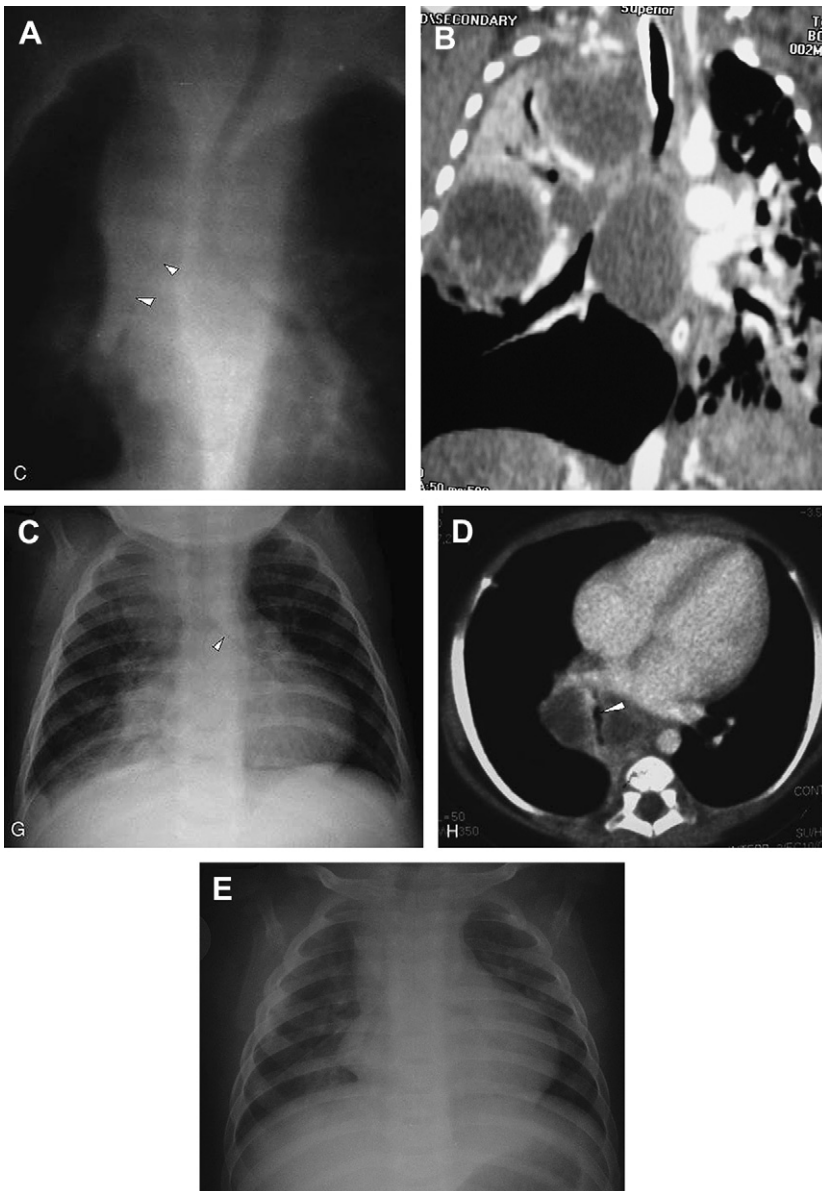


**Fig. 29.** Airway compression. (A) Cropped and contrast manipulated view of the airway in a child showing significant compression of the right main bronchus and bronchus intermedius (*arrowheads*) and less obvious compression of the left main bronchus by TB lymphadenopathy. (B) Coronal reformat of a contrast-enhanced CT of the chest in a child showing the significant airway compression of the right main bronchus and bronchus intermedius by massive rim-enhancing TB lymphadenopathy. (C) Chest radiograph shows complete obliteration of the right main bronchus and bronchus intermedius with resultant right upper lobe and right middle lobe parenchymal lung disease in addition to partial compression of the left main bronchus (*arrowhead*). (D) Corresponding CT of the patient in (C) shows the offending lymphadenopathy and the severe compression of the bronchus intermedius (*arrowhead*). (E) Follow-up radiograph of the patient in (C) after surgical enucleation of the right hilar and subcarinal lymphadenopathy shows reconstitution of the caliber of right- and left-sided airways and resolution of the parenchymal disease. (Parts (A), (C) and (D) from Andronikou S, Wieselthaler N. Imaging for tuberculosis in children. In: Schaaf HS, Zumla A, editors. Tuberculosis: a comprehensive clinical reference. Philadelphia: Saunders Elsevier; 2009. p. 272–3; with permission.)

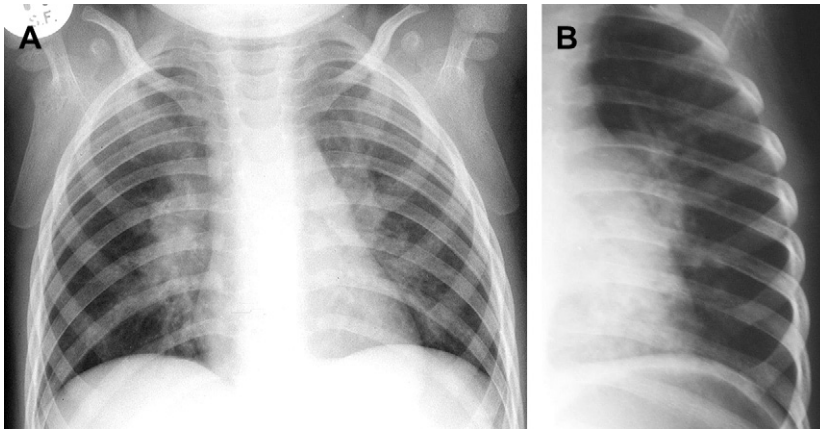


**Fig. 30.** Lymphadenopathy. (A) There is a lobulated mass projecting beyond the cardiac margin on the right at the hilum in keeping with hilar lymphadenopathy. (B) A cropped image of the left chest shows a lobulated mass at the left hilum projecting beyond the cardiac margin in keeping with lymphadenopathy. In addition, there is air-space disease posterior to the heart.

#### **CT and MRI**

Single or multiple cardiac tuberculomas may be shown as sharply demarcated lesions especially involving the right heart chambers. CT shows calcification more successfully<sup>44</sup> with or without thrombus formation, which may extend into the vena cava.<sup>45</sup>

#### **Acute Respiratory Distress Syndrome**

Acute respiratory distress syndrome may result as an evolution of miliary TB.

#### **CXR**

A “snow-storm” appearance is characteristic. After recovery, multiple cystic lesions (pneumatoceles or bullae) may remain.

#### **Broncholithiasis**

Broncholithiasis is an uncommon complication occurring after rupture of a calcified peribronchial lymph node into a bronchus.<sup>46</sup>

#### **CT**

CT shows the calcified lymph node associated with bronchial obstruction, atelectasis, obstructive pneumonitis, branching calcification, focal hyperinflation, or bronchiectasis.<sup>12</sup>

#### **Fibrosing Mediastinitis**

This uncommon complication arises after coalescence of multiple mediastinal lymph nodes and multiple tuberculomas creating an acute inflammatory reaction and reactive fibrosis.

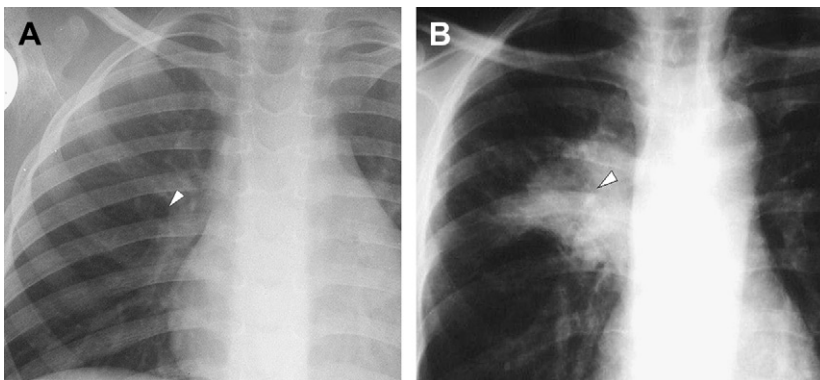


**Fig. 31.** Hilar point and lymphadenopathy. (A) Cropped radiograph of the right chest shows the right hilum where large upper zone and large lower zone vessels meet (arrowhead). This normal hilar point is outwardly concave and appears like a horizontally oriented V. (B) On the right there is filling in of the horizontal V, which is just visible (arrowhead) through the mass of TB lymph nodes.

**CT**

A mediastinal and hilar mass with calcification, tracheobronchial narrowing, and vascular encasement (and in some cases superior vena cava syndrome) are evident.<sup>47</sup>

**Pneumothorax**

Pneumothorax may complicate severe cavitary disease and heralds the onset of a bronchopleural fistula.<sup>12</sup>

**CXR and CT**

A crescent of air (with no discernable lung markings) is seen in the nondependent portion of the chest (erect, apicolateral; supine, inferiorly and medial). There may be mass effect phenomena on the mediastinum when the pneumothorax is large.

**Esophageal TB and Tracheo-esophageal Fistula**

Esophageal TB is more common in patients infected with HIV.<sup>48</sup> It results from ingestion of

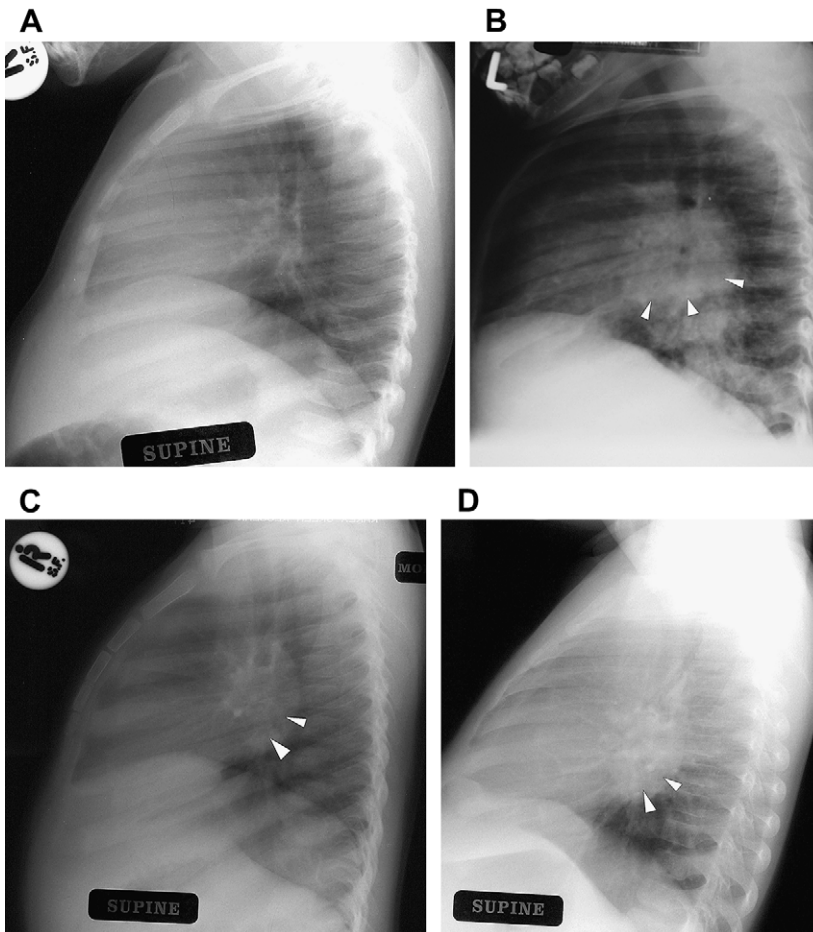


**Fig. 32.** Lateral radiographs. (A) A normal lateral radiograph shows no oval densities behind the trachea/bronchus intermedius or below its apparent termination. The density of the main pulmonary arteries and posterior aspect of the aortic arch are visible. (B) Obvious lymphadenopathy on a lateral radiograph is shown as oval densities posterior and inferior to the trachea/bronchus intermedius (*arrowheads*). Associated with the normal dense structures more superiorly, this fits the description known as the “doughnut sign”. There is also lower lobe consolidation projected over the distal visible vertebral bodies. (C) Oval density representing subcarinal lymphadenopathy is noted posterior and inferior to the trachea/bronchus intermedius (*arrowheads*). (D) Another example where oval density representing subcarinal lymphadenopathy is noted posterior and inferior to the trachea/bronchus intermedius (*arrowheads*). (E) Multiplanar CT reconstruction with cross-hair cross-referencing used to show the positional projection of subcarinal and hilar lymphadenopathy on a lateral radiograph, by inference from the sagittal reconstruction (*top right corner*). (F) Sagittal STIR/T2 MRI shows the hilar mass of low signal TB lymph nodes (*large arrowhead*) which would be shown as a doughnut on a lateral image. On MRI the triad of normal vessels that form the superior aspect of the doughnut show flow void (*small arrowheads*).

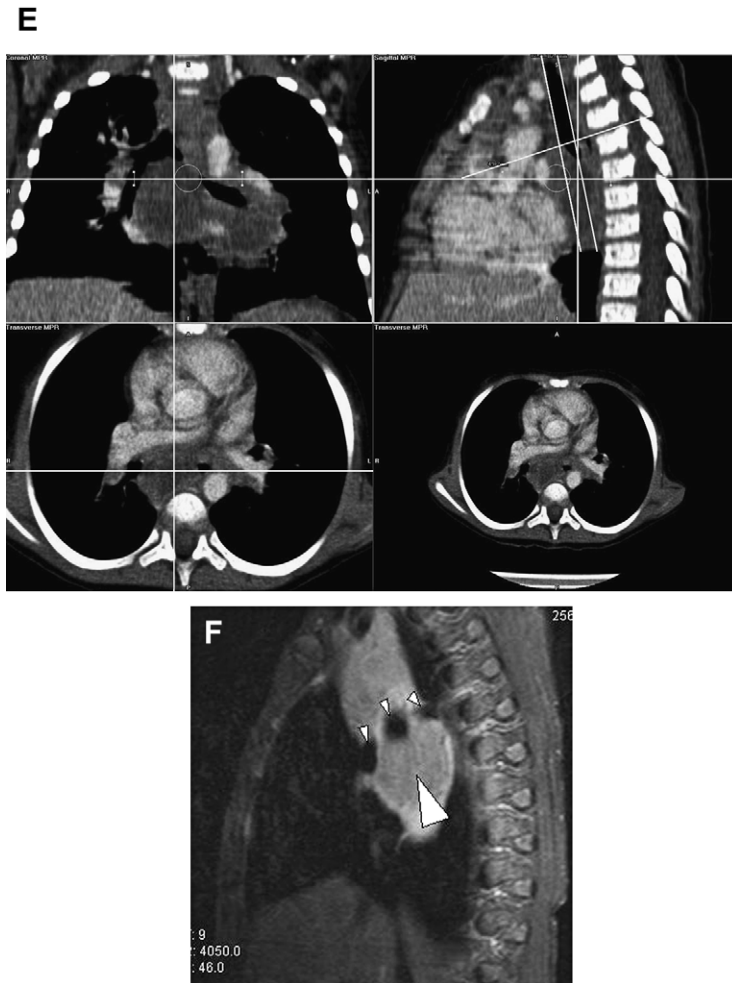


Fig. 32. (continued)

infected sputum (intrinsic), spread from an adjacent TB lymph node or pulmonary TB (extrinsic) or may be the result of hematogenous or lymphatic spread.<sup>49</sup>

### Barium study

Barium studies show narrowing and displacement, often at the subcarinal level caused by proximity of the esophagus to the lymphadenopathy in this region. Advanced disease results in esophageal ulceration, fistula formation, stricture, and traction diverticula (Fig. 27A).<sup>48,49</sup> Tracheo-esophageal fistula may develop and is shown with contrast in the airways (in the absence of aspiration) (Fig. 27B).<sup>50</sup>

### CT

The extent of disease and the extrinsic causes may be evident.

### Chylous Effusion

This is an extremely rare complication described in children caused by infiltration or compression of the thoracic duct by right paratracheal lymphadenopathy. The chylous nature of the effusion is best determined with an aspirate.

### US and CT

Large effusions are shown either uni- or bilaterally (10–20 HU). The enlarged lymph nodes in the right paratracheal and other locations may be a clue to TB as the cause.<sup>51</sup>

### Phrenic Nerve Palsy

This is a rare complication reported in children. Large lymphadenopathy in the AP window causes compression and infiltration of the phrenic nerve causing diaphragmatic paralysis.<sup>52</sup>

**CXR and CT**

The elevated hemidiaphragm is always on the left. Usually there is accompanying left-sided consolidation with volume loss. On CT this is shown to be caused by compression of the left main bronchus. This is not only caused by lymphadenopathy but also because the mediastinum is displaced to the right allowing the displaced aorta to contribute to the compression of the bronchus.<sup>52</sup>

**Chest Wall TB**

The ribs are a frequent location for involvement of tuberculous osteomyelitis. TB granulomatous inflammation and abscesses of the chest wall are most commonly found at the parasternal region,

costovertebral junction, and along the shafts of the ribs. It is thought that lymph node enlargement and subsequent caseation necrosis may burrow through the chest wall.<sup>53</sup>

**CXR and CT**

CT is more accurate to show subtle rib involvement than CXR. There is usually associated TB pleuritis and intrathoracic lymph node enlargement in contiguity with these chest wall collections. The internal mammary nodes are most commonly involved.

**MRI**

MRI is the preferred imaging method to assess isolated pyomyositis of the chest wall. The lesion

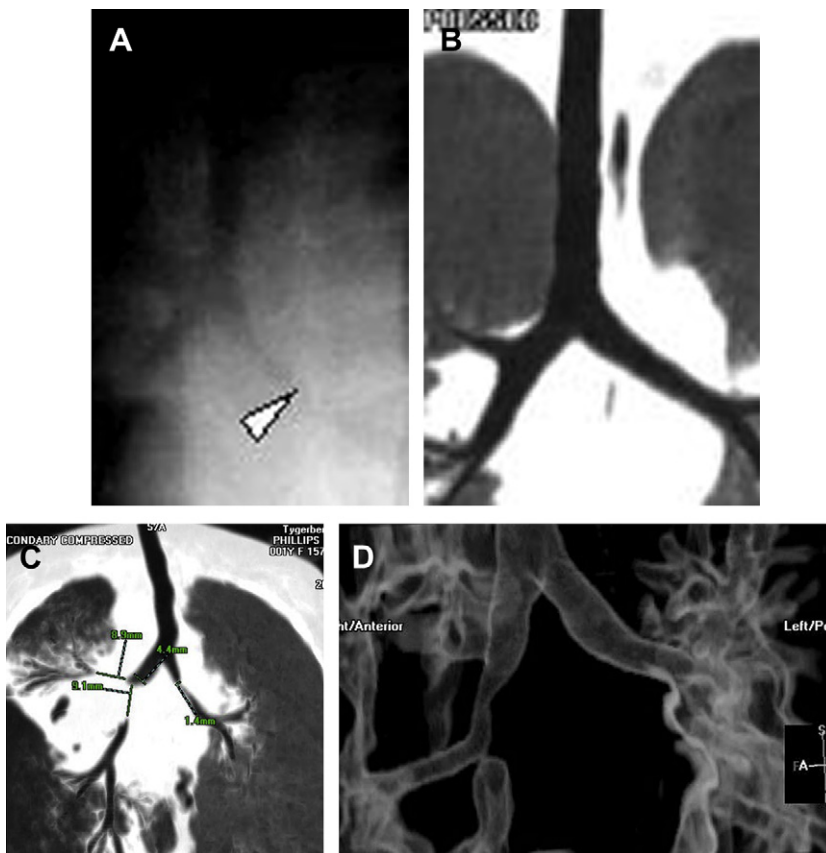


**Fig. 33.** Techniques for showing the airway. (A) High kilovolt radiographs used to better show airway stenosis of the left main bronchus (arrowhead). (From Andronikou S, Wieselthaler N. Imaging for tuberculosis in children. In: Schaaf HS, Zumla A, editors. Tuberculosis: a comprehensive clinical reference. Philadelphia: Saunders Elsevier; 2009. p. 272; with permission.) (B) Thick slab minimum intensity projection CT reconstruction shows a normal airway caliber and outline. (C) Thick slab minimum intensity projection CT reconstruction shows how the technique is used to identify stenoses caused by TB and show their length (an advantage over bronchoscopy when the scope cannot pass a compressed area). (D) Three-dimensional volume rendered CT reconstruction technique with transparent setting. The bronchus intermedius and right lower lobe bronchus narrowing are well shown. (From du Plessis J, Goussard P, Andronikou S, Gie R, George R. Comparing three-dimensional volume-rendered CT images with fiberoptic tracheobronchoscopy in the evaluation of airway compression caused by tuberculous lymphadenopathy in children. *Pediatr Radiol* 2009;39(7):696; with kind permission of Springer Science + Business Media.)

is of low signal intensity on T1-weighted images and of high signal intensity on T2-weighted images. There is marked contrast enhancement after intravenous administration of gadolinium (**Fig. 28**). Abscess formation is the rule in all cases of advanced pyomyositis. The peripheral wall of the abscess shows a subtle hyperintensity on T1-weighted images and hypointensity on T2-weighted images. On gadolinium-enhanced images, a peripheral enhancing rim corresponding to the abscess wall is observed.

### **Vascular**

Pulmonary arteries and veins in an area of active TB may show vasculitis and thrombosis. Bronchial arteries may be enlarged in TB bronchiectasis or parenchymal TB. Rasmussen aneurysms, which are pseudoaneurysms of the pulmonary arteries occurring adjacent to TB cavities, occur in 5% of patients.<sup>54</sup> Hemoptysis is the usual presentation and it ranges from being minimal to massive and life-threatening.

### **CXR and CT**

Nodular and tubular structures are seen adjacent to areas of bronchiectasis.

### **CT angiography**

CT angiography is useful for confirming that tubular structures on CXR are ectatic vessels.

### **Angiographic arterial embolization**

Angiographic arterial embolization achieves control of massive hemoptysis while awaiting definitive therapy.

## **IMAGING TIPS AND NOVEL IDEAS**

### **Tips for Reading Chest Radiographs**

#### **AP CXR in children**

- The most important feature to detect is airway displacement or compression. This may be an indirect sign of lymphadenopathy but is the most objective radiological sign as the airway is the only discernable structure within the density of the mediastinum (**Fig. 29A**).<sup>14</sup> Airways in normal children are compressible and the normal trachea should be positioned to the right of the midline. Normal bronchi should taper distally and should also be of similar size at an equal distance from the carina on both sides. Lymphadenopathy causes compression of the major airways and may displace the trachea to the left (**Fig. 29B**).<sup>10,14,55</sup> Offending lymphadenopathy can be enucleated to relieve the obstruction and allow re-expansion of the lung (**Fig. 29C–E**).

- The lobulated soft tissue masses of lymphadenopathy at the paratracheal region and hilar regions are often hidden behind the thymic shadow or the heart shadow, which is relatively large in children. Noting only the outwardly convex lobulated masses that extend beyond the cardiac margin ensures that only definite lymphadenopathy is recorded (**Fig. 30**).

#### **PA CXR in adults**

Lymphadenopathy is represented by a polycyclic, curvilinear or lobulated outline to the mediastinum.<sup>56</sup> Enlarged paratracheal or pretracheal lymph nodes result in widening or obliteration of the right paratracheal stripe within a wide mediastinum.<sup>56</sup> A normal hilar point should show a V on its side, convex outward (**Fig 31A**). Filling of this point, failure to identify it, or an outwardly convex or lobulated margin may represent a mass, including lymphadenopathy (**Fig. 31B**).

#### **Lateral CXR in children**

Subcarinal and retrocarinal lymphadenopathy is represented as a lobulated density inferior and posterior to the bronchus intermedius.<sup>56</sup> Lymphadenopathy in this region completes the lower half of a doughnut-shaped density (the upper half of which is made up of the right and left main pulmonary arteries and aortic arch) (**Fig. 32**).<sup>14</sup>

### **Advanced Airway Assessment (High Kilovolt, Three-dimensional Reconstruction, Virtual Bronchoscopy)**

Use of high kilovolt radiographs using a filter technique is not recommended for routine use but can assist in showing the airway, which if compressed or displaced strongly suggests lymphadenopathy (**Fig. 33A**).<sup>55</sup> In more advanced departments, reconstruction of multidetector CT (MDCT) is



**Fig. 34.** Axillary lymphadenopathy. STIR/T2 MRI shows the large axillary lymph nodes (arrowheads) in this patient with mediastinal and hilar TB lymphadenopathy.

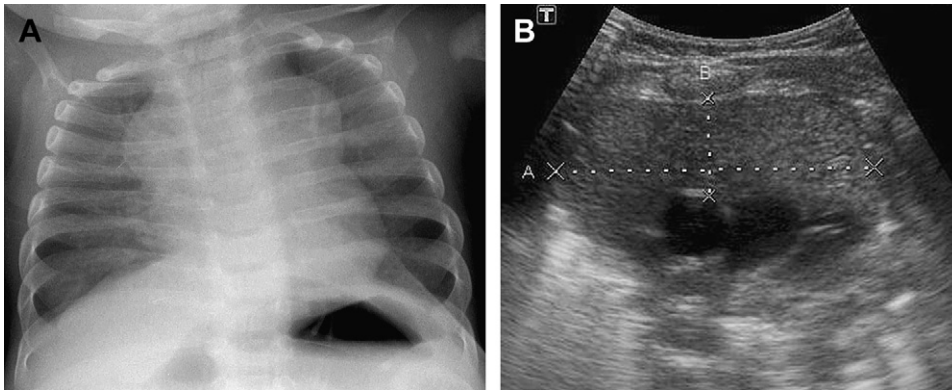


**Fig. 35.** Thymus. (A) Plain radiograph shows how the normal thymus can cause the mediastinum to appear wide and have outwardly convex margins. There is no displacement or compression of mediastinal structures by normal thymic tissue. (B) When there is doubt about a mediastinal width, suggesting lymphadenopathy or a mass, ultrasound is useful to show the homogenous texture of the normal thymus seen here (as opposed to the nodular heterogeneous appearance of a mass or lymphadenopathy).

possible in many ways including minimum intensity projections (Fig. 33B, C), volume rendered three-dimensional (Fig. 33D) and virtual bronchoscopy. The three-dimensional volume rendered technique has been assessed against bronchoscopy for detection and characterization of the airway and the causative extrinsic mass. The CT technique was shown to not only match bronchoscopy but also to assess the degree of compression more accurately, and managed to show more distal obstructions of bronchi where the bronchoscope could not navigate because of proximal obstruction.<sup>10</sup> Bronchoscopy can be reserved for when biopsy may be necessary.

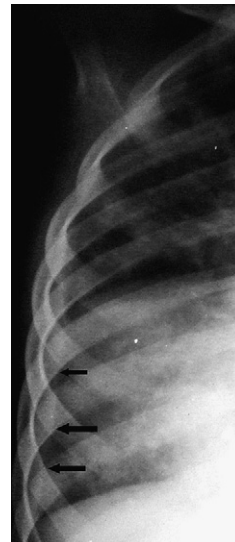
#### **Routine Availability of HRCT with MDCT (Combi-scanning)**

Current MDCT scanning produces slices thin enough to be useful as high-resolution imaging (after reconstruction with appropriate filters). This means that every time an MDCT is performed with contrast for visualization of mediastinal nodes, effusions, air-space disease, and other complications of TB, the data set is available for reconstruction and review as an HRCT study. This is useful for detecting miliary and other interstitial nodules (and lines), bronchiectasis, tree-in-bud features of bronchogenic spread, and air-filled cysts. This is known to add to the diagnostic confidence in TB assessment and the determination of outcome, and can affect management (eg, detection of cavities and bronchiectasis).<sup>57</sup> The converse is also possible; that is, when clinicians request HRCT for TB, the study should be performed as a postcontrast, thin-slice mediastinal study (combi-scan) and the HRCT component

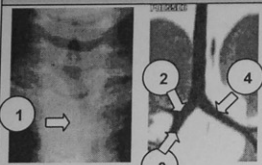
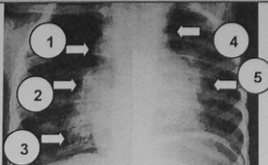
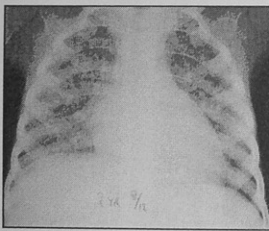
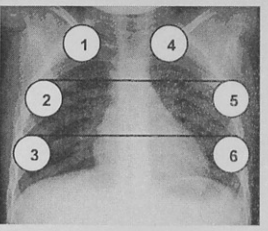
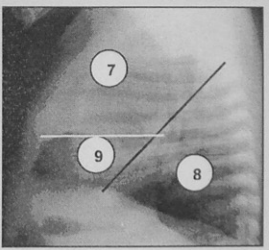
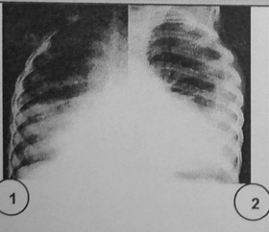
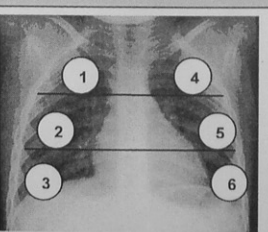
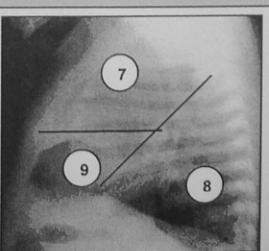
can be produced in addition to the mediastinal window with a comment on the presence of lymphadenopathy and other information.

#### **Ultrasound for Diagnosis**

Ultrasound has been used successfully to detect mediastinal lymphadenopathy via the suprasternal and parasternal approaches in children.<sup>58</sup> Follow-up



**Fig. 36.** Cropped plain radiograph of the right chest to show how effusion, termed laminar effusions, in children spares the costophrenic angle and tracks superiorly along the lateral chest wall. A tip for detecting these is to check that the lung reaches the rib margins. In normal children there are no significant companion shadows and when a linear density separates the ribs from the lung an effusion is suspected.

<b>INFORMATION:</b>							
• Reader code: ..... • Patient code: .....	• Study code: ..... • Date of read: .....						
<b>Instructions to tick-sheet:</b> A) Mark <b>only one</b> of the tick boxes for each image: <input type="checkbox"/> Yes, <input type="checkbox"/> No, <input type="checkbox"/> Maybe, or <input type="checkbox"/> Not visible (Record <b>only the most positive grading</b> under each section. That means if there is one 'definite' node and 3 'possible' nodes, you must tick 'yes' and not 'maybe') B) Please <b>also</b> cross any number of locations of disease on the appropriate circled number		<b>Grading:</b> Yes = positive Maybe No = negative <div style="text-align: right; border-left: 1px solid black; height: 40px; margin-left: 5px;"></div>					
<b>Airway compressed and tracheal displacement</b>  <div style="display: flex; align-items: center;"> <div style="writing-mode: vertical-rl; transform: rotate(180deg); font-weight: bold; margin-right: 5px;">Lymphadenopathy</div>  </div> <p>1 = compressed Or displaced to left only      2-4=compression</p>	<b>Soft tissue density = nodal mass</b>  <div style="display: flex; align-items: center;">  </div>	<b>Post process: Overall</b>  <table border="1" style="width: 100%; border-collapse: collapse;"> <tr><td style="text-align: center;">Lymphadenopathy</td></tr> <tr><td style="text-align: center;">Yes</td></tr> <tr><td style="text-align: center;">No</td></tr> <tr><td style="text-align: center;">Maybe</td></tr> <tr><td style="text-align: center;">Not visible</td></tr> </table>	Lymphadenopathy	Yes	No	Maybe	Not visible
Lymphadenopathy							
Yes							
No							
Maybe							
Not visible							
<input type="checkbox"/> Yes <input type="checkbox"/> No <input type="checkbox"/> Maybe <input type="checkbox"/> Not visible	<input type="checkbox"/> Yes <input type="checkbox"/> No <input type="checkbox"/> Maybe <input type="checkbox"/> Not visible	<input type="checkbox"/> Yes <input type="checkbox"/> No <input type="checkbox"/> Maybe <input type="checkbox"/> Not visible					
<b>Nodular = Millitary or larger widespread and bilateral</b>  	<b>Airspace consolidation</b>  <div style="display: flex; align-items: center;">   </div> <p style="text-align: center; font-size: small;">Lines indicate the trachea</p>	<b>Post process: Overall</b>  <table border="1" style="width: 100%; border-collapse: collapse;"> <tr><td style="text-align: center;">Lung disease</td></tr> <tr><td style="text-align: center;">Yes</td></tr> <tr><td style="text-align: center;">No</td></tr> <tr><td style="text-align: center;">Maybe</td></tr> <tr><td style="text-align: center;">Not visible</td></tr> </table>	Lung disease	Yes	No	Maybe	Not visible
Lung disease							
Yes							
No							
Maybe							
Not visible							
<input type="checkbox"/> Yes <input type="checkbox"/> No <input type="checkbox"/> Maybe <input type="checkbox"/> Not visible	<input type="checkbox"/> Yes <input type="checkbox"/> No <input type="checkbox"/> Maybe <input type="checkbox"/> Not visible	<input type="checkbox"/> Yes <input type="checkbox"/> No <input type="checkbox"/> Maybe <input type="checkbox"/> Not visible					
<b>Pleural effusion/thickening</b>  	<b>Cavities</b>  <div style="display: flex; align-items: center;">   </div>	<b>Post process: Overall</b>  <table border="1" style="width: 100%; border-collapse: collapse;"> <tr><td style="text-align: center;">Pleura</td></tr> <tr><td style="text-align: center;">Yes</td></tr> <tr><td style="text-align: center;">No</td></tr> <tr><td style="text-align: center;">Maybe</td></tr> <tr><td style="text-align: center;">Not visible</td></tr> </table>	Pleura	Yes	No	Maybe	Not visible
Pleura							
Yes							
No							
Maybe							
Not visible							
<input type="checkbox"/> Yes <input type="checkbox"/> No <input type="checkbox"/> Maybe <input type="checkbox"/> Not visible	<input type="checkbox"/> Yes <input type="checkbox"/> No <input type="checkbox"/> Maybe <input type="checkbox"/> Not visible	<input type="checkbox"/> Yes <input type="checkbox"/> No <input type="checkbox"/> Maybe <input type="checkbox"/> Not visible					
<b>TB Decision</b>							
<input type="checkbox"/> Lymphadenopathy or Millitary = <b>Yes</b>	<input type="checkbox"/> No lymphadenop/mill but positive = <b>Maybe</b>	<input type="checkbox"/> Normal = <b>NO</b>	<input type="checkbox"/> Bad quality = <b>Unreadable</b>				

**Fig. 37.** A tick sheet designed for use in children investigated for TB to record information in a retrievable manner and to ensure that the correct aspects of diagnosis are reviewed by the readers in order of priority. (Courtesy of S. Moyo, M. Hatherill, and the South African Tuberculosis Vaccine Initiative, Cape Town, South Africa; with permission.)

ultrasound using the same method has successfully showed response to therapy with decrease in size or disappearance of lymphadenopathy.<sup>59</sup> Using ultrasound to diagnose pulmonary TB by identifying associated abdominal lymphadenopathy has been suggested but shown to be positive in only 25% of patients.<sup>60</sup> The increasing incidence of extrapulmonary TB may make this more important over time especially when used to additionally detect axillary lymphadenopathy (**Fig. 34**) (shown to have a moderate correlation with the presence of intrathoracic lymphadenopathy using CT<sup>61</sup>) and cervical lymphadenopathy. Fine-needle aspiration biopsy can be guided by ultrasound in various locations including the mediastinum.<sup>62</sup>

## CONSIDERATIONS IN CHILDREN

### *Thymus*

The mediastinum on CXR in children less than 5 years of age shows a prominent thymus that can be as wide as the thoracic cavity. Even though it may have a variable size, margin, and appearance, the thymus is a soft organ and never displaces or compresses the airways (unless infiltrated and abnormal or replaced by lymphadenopathy) (**Fig. 35A**). Suprasternal ultrasound, CT or MRI can identify normal thymic tissue (**Fig. 35B**) and distinguish it from lymphadenopathy.

### *Heart*

The heart occupies a larger proportion of the chest in a child than in an adult. This masks the hila making it difficult to evaluate the hilar points for lymphadenopathy as described in adults. Instead of considering this a disadvantage, identification of lobulated shadows projecting beyond the cardiac margins should add confidence to the certainty of the presence of lymphadenopathy.

### *Trachea and Bronchi*

Children have soft and compressible airways, which results in the complication of lymphobronchial TB (with compression and distal parenchymal disease) more often than in adults. However, the compressibility of the airways can be used to advantage to infer the presence of lymphadenopathy when noted on CXR.

### *Effusions*

In children, effusions seen on CXR tend to spare the costophrenic angle and extend cranially along the lateral chest wall as they increase in amount. They are termed lamellar effusions and should be checked by looking for a linear density separating the air-filled edge of lung from the lateral chest wall

(**Fig. 36**). Children lack the soft tissue companion shadows noted in adults that would be difficult to distinguish from this imaging pattern.

### *Radiation*

Children are more vulnerable to radiation from medical investigations because of the immature developing organs, the close proximity of sensitive areas (shorter bodies), and the longer life ahead in which to develop malignancies. The lateral CXR is not only an additional view but it imparts approximately twice the radiation dose of the AP CXR. However, the dose is relatively low compared with traditional CT, which is equivalent to approximately 100 CXR. Modern departments have reduced CT doses dramatically by decreasing the tube current setting.<sup>63</sup>

### *Lymphadenopathy: What Size is Abnormal?*

This is a relevant question that has been raised regarding chest CT imaging for TB in children<sup>64</sup> but has also been addressed with regard to abdominal lymphadenopathy in children.<sup>65</sup> Because normal children have been shown to have lymphadenopathy up to 5 mm, the authors recommend noting only lymphadenopathy greater than 1 cm unless there is clear central necrosis on CT, calcification, or low signal intensity on T2-weighted MRI images.

## RECORDING SYSTEMS AND TICK SHEETS

Many recording systems have been devised to assist recording of features of TB (**Fig 37**), particularly for the purposes of research, screening, and data collection. These systems not only ensure that a systematic approach is followed but also systematic recording of the findings using a common language. This makes reporting applicable for follow-up especially if this is not always by the same physician or radiologist. These systems are useful for training residents and non-radiologists in identifying and recording the pertinent features of TB in an organized fashion. Testing of 1 such tick sheet has suggested that CXR may be more useful as a screening tool for TB than previously recognized.<sup>66</sup>

## SUMMARY

This article reviews the ongoing role of imaging in the diagnosis of TB and its complications. The blurring of differences in the presentation patterns must be absorbed into daily practice. Communication between radiologists and clinicians and improved interpretation skills by clinicians is increasingly important in the field for making

management decisions, especially where there are limited resources. Recognition of special imaging, anatomic, and vulnerability differences between children and adults is more important than trying to define patterns of disease exclusive to children. Most importantly, radiologists must continue to push ahead with research into identifying more accurate and cheaper methods of diagnosing TB. Even though some aspects of imaging are being discredited, they persist in practice because laboratory and clinical tests have been disappointing or unaffordable. High-end imaging should be used to confirm the most confident and reliable aspects of diagnosis on cheaper modalities such as plain radiographs. These can then be used with greater confidence in the less fortunate parts of the world that suffer the most from this disease.

### ACKNOWLEDGMENT

The authors wish to thank Paul Van den Brande, MD, PhD, for his contribution in the preparation of this manuscript.

### REFERENCES

1. Reid MJA, Shah NS. Approaches to tuberculosis screening and diagnosis in people with HIV in resource-limited setting. *Lancet Infect Dis* 2009;9:173–84.
2. Zellweger JP, Heinzer R, Touray M, et al. Intra-observer and overall agreement in the radiological assessment of tuberculosis. *Int J Tuberc Lung Dis* 2006;10:1123–6.
3. Swingler GH, du Toit G, Andronikou S, et al. Diagnostic accuracy of chest radiography in detecting mediastinal lymphadenopathy in suspected pulmonary tuberculosis. *Arch Dis Child* 2005;90(11):1153–6.
4. Marais BJ, Parker SK, Verver S, et al. Primary and postprimary or reactivation tuberculosis: time to revise confusion terminology? *AJR Am J Roentgenol* 2009;192(4):W198 [author reply W199–200].
5. Stead WW. Tuberculosis among elderly persons, as observed among nursing home residents. *Int J Tuberc Lung Dis* 1998;2:S64–70.
6. Van Rie A, Warren R, Richardson M, et al. Exogenous reinfection as a cause of recurrent tuberculosis after curative treatment. *N Engl J Med* 1999;341:1174–9.
7. Verver S, Warren RM, Munch Z, et al. Proportion of tuberculosis transmission that takes place in households in a high-incidence area. *Lancet* 2004;363:212–4.
8. Verver S, Warren RM, Beyers N, et al. Rate of reinfection tuberculosis after successful treatment is higher than rate of new tuberculosis. *Am J Respir Crit Care Med* 2005;171:1430–5.
9. Hamilton CD, Stout JE, Goodman PC, et al. The value of the end-of-treatment chest radiograph in predicting pulmonary TB relapse. *Int J Tuberc Lung Dis* 2008;12:1059–64.
10. du Plessis J, Goussard P, Andronikou S, et al. Comparing three-dimensional volume-rendered CT images with fiberoptic tracheobronchoscopy in the evaluation of airway compression caused by tuberculous lymphadenopathy in children. *Pediatr Radiol* 2009;39(7):694–702.
11. De Backer AI, Vanhoenacker FM, Van den Brande P. Computed tomography, magnetic resonance imaging and PET in tuberculosis. In: Schaaf HS, Zumla A, editors. *Tuberculosis: a comprehensive clinical reference*. Philadelphia: Saunders Elsevier; 2009. p. 296–314.
12. Van Dyck P, Vanhoenacker FM, Van den Brande P, et al. Imaging of pulmonary tuberculosis. *Eur Radiol* 2003;13(8):1771–85.
13. Woodring JH, Vandiviere HM, Lee C. Intrathoracic lymphadenopathy in post-primary TB. *South Med J* 1988;81:992–7.
14. Andronikou S, Wieselthaler N. Modern imaging of tuberculosis in children: thoracic, central nervous system and abdominal tuberculosis. *Pediatr Radiol* 2004;34(11):861–75 [Epub 2004 Sep 15].
15. Lighter J, Rigaud. Diagnosing childhood TB: traditional and innovative modalities. *Curr Probl Pediatr Adolesc Health Care* 2009;39:61–88.
16. Kim WS, Moon WK, Kim IO, et al. Pulmonary tuberculosis in children: CT evaluation. *AJR Am J Roentgenol* 1997;168:1005–9.
17. Jeong YJ, Lees KS. Pulmonary tuberculosis: up-to-date imaging and management. *Am J Roentgenol* 2008;191:834–44.
18. Hartman TE, Primack SL, Muller NL, et al. Diagnosis of thoracic complications in AIDS: accuracy of CT. *Am J Roentgenol* 1994;162:547–53.
19. Leung AN, Muller NL, Pineda PR, et al. Primary tuberculosis in childhood: radiographic manifestations. *Radiology* 1992;182:87–91.
20. Hopewell PC. A clinical view of tuberculosis. *Radiol Clin North Am* 1995;33:641–53.
21. Available at: [http://www.lumrix.net/medical/radiology/tuberculosis\\_radiology.html](http://www.lumrix.net/medical/radiology/tuberculosis_radiology.html). Accessed July 4, 2009.
22. Yilmaz MU, Kumcuoglu Z, Utkaner G, et al. CT findings of tuberculous pleurisy. *Int J Tuberc Lung Dis* 1998;2:164–7.
23. Goodman PC. Pulmonary tuberculosis in patients with acquired immunodeficiency syndrome. *J Thorac Imaging* 1990;5:38–45.
24. Wall SD, Edinburgh KJ. Invited commentary. Abdominal findings in AIDS-related pulmonary tuberculosis correlated with associated CD4 levels. *Abdom Imaging* 1998;23:578–9.

25. Perlman DC, el-Sadr WM, Nelson ET, et al. Variation of chest radiographic patterns in pulmonary tuberculosis by degree of HIV-related immunosuppression. The Terry Beinr Community Programs for Clinical Research on AIDS (CPCRA). The AIDS Clinical Trials Group (ACTG). *Clin Infect Dis* 1997;25:242–56.
26. Haramati LB, Jenny-Avital ER, Alterman DD. Effect of HIV status on chest radiographic and CT findings in patients with tuberculosis. *Clin Radiol* 1997;52:31–5.
27. Raviglione MC, Narain JP, Kochi A. HIV-associated tuberculosis in developing countries: clinical features, diagnosis and treatment. *Bull World Health Organ* 1992;70:515–26.
28. Buckingham SJ, Haddow LJ, Shaw PJ, et al. Immune reconstitution inflammatory syndrome in HIV-infected patients with mycobacterial infections starting highly active anti-retroviral therapy. *Clin Radiol* 2004;59(6):505–13.
29. Nakanishi M, Demura Y, Ameshima S, et al. Utility of high-resolution computed tomography for predicting risk of sputum smear-negative pulmonary tuberculosis. *Eur J Radiol* 2009. Jan 22 [Epub ahead of print].
30. Griffith-Richards SB, Goussard P, Andronikou S, et al. Cavitating pulmonary tuberculosis in children: correlating radiology with pathogenesis. *Pediatr Radiol* 2007;37(8):798–804 [quiz 848–9. Epub 2007 May 26].
31. Andronikou S, Joseph E, Lucas S, et al. CT scanning for the detection of tuberculous mediastinal and hilar lymphadenopathy in children. *Pediatr Radiol* 2004;34(3):232–6.
32. Maydell AT, Goussard P, Andronikou P. Radiological changes post lymph node enucleation for airway obstruction in children with pulmonary TB. *Pediatr Radiol* 2009;39(Suppl 3):517.
33. Andronikou S, Wieslthaler N. Imaging for tuberculosis in children. In: Schaaf HS, Zumla A, editors. *Tuberculosis: a comprehensive clinical reference*. Philadelphia: Saunders Elsevier; 2009. p. 261–95.
34. Lee KS, Kim YH, Kim WS, et al. Endobronchial tuberculosis: CT features. *J Comput Assist Tomogr* 1991;15:424–8.
35. Moon WK, Im JG, Yeon KM, et al. Tuberculosis of central airways: CT findings of active and fibrotic disease. *Am J Roentgenol* 1997;169:649–53.
36. Kim Y, Song KS, Goo JM, et al. Thoracic sequelae and complications of tuberculosis. *Radiographics* 2001;21:839–58.
37. Im JG, Itoh H, Han MC. CT of pulmonary tuberculosis. *Semin Ultrasound CT MR* 1995;16:420–34.
38. Glicklich M, Mendelson DS, Gendal ES, et al. Tuberculous empyema necessitatis: CT findings. *Clin Imaging* 1990;14:23–5.
39. Westcott JL, Volpe JP. Peripheral bronchopleural fistula: CT evaluation in 20 patients with pneumonia, empyema or postoperative air leak. *Radiology* 1995;196:175–81.
40. Fraser RS. Pulmonary aspergillosis: pathologic and pathogenetic features. *Pathol Annu* 1993;28:231–77.
41. Ahmad A, Ellis J, Nesbitt A, et al. Pericardial effusions in children with severe protein energy malnutrition resolve with therapeutic feeding: a prospective cohort study. *Arch Dis Child* 2008;93:1033–6.
42. Casas E, Blanco JR, Ibara V, et al. Incidence of pericardial effusion in pulmonary tuberculosis. *Int J Tuberc Lung Dis* 2000;4:1172–5.
43. Burrill J, Williams CJ, Bain G, et al. Tuberculosis: a radiologic review. *Radiographics* 2007;27(5):1255–73.
44. Rodriguez E, Soler R, Juffé A, et al. CT and MR findings in a calcified myocardial tuberculoma of the left ventricle. *J Comput Assist Tomogr* 2001;25:577–9.
45. Al-Nasser I, Anwar AM, Nosir YF, et al. Bicaval obstruction complicating right atrial tuberculoma: the diagnostic value of cardiovascular MR. *J Cardiovasc Magn Reson* 2008;10(1):60.
46. Conces DJ Jr, Tarver RD, Vix VA. Broncholithiasis: CT features in 15 patients. *Am J Roentgenol* 1991;157:249–53.
47. Lee JY, Kim Y, Lee KS, et al. Tuberculous fibrosing mediastinitis: radiological findings. *Am J Roentgenol* 1996;167:1598–9.
48. Vanhoenacker FM, De Backer AI, Op de Beeck B, et al. Imaging of gastrointestinal and abdominal tuberculosis. *Eur Radiol* 2004;14:E103–15.
49. De Backer AI, Mortelé KJ, De Keulenaer BL, et al. CT and MRI of gastrointestinal tuberculosis. *JBR-BTR* 2006;89:190–4.
50. Erlank A, Goussard P, Andronikou S, et al. Oesophageal perforation as a complication of primary pulmonary tuberculous lymphadenopathy in children. *Pediatr Radiol* 2007;37(7):636–9.
51. Grobbelaar M, Andronikou S, Goussard P, et al. Chylothorax as a complication of pulmonary tuberculosis in children. *Pediatr Radiol* 2008;38(2):224–6.
52. Goussard P, Gie RP, Kling S, et al. Phrenic nerve palsy in children associated with confirmed intrathoracic tuberculosis: diagnosis and clinical course. *Pediatr Pulmonol* 2009;44(4):345–50.
53. Morris BS, Maheshwari M, Chalwa A. Chest wall tuberculosis: a review of CT appearances. *Br J Radiol* 2004;77:449–57.
54. Santelli ED, Katz DS, Goldschmidt AM, et al. Embolization of multiple Rasmussen aneurysms as a treatment of hemoptysis. *Radiology* 1994;193:396–8.
55. De Villiers RV, Andronikou S, Van de Westhuizen S. Specificity and sensitivity of chest radiographs in the diagnosis of paediatric pulmonary tuberculosis and the value of additional high-kilovolt radiographs. *Australas Radiol* 2004;48(2):148–53.

56. Neufang KFR, Beyer D, Peters PE. Conventional Roentgen diagnosis of mediastinal lymphadenopathy. Review article (Part 1). *Lymphology* 1982;4:132–42.
57. Erlank A, Andronikou S, Ackermann C, et al. Does the routine availability of a high-resolution CT (multi-detector CT) on the chest in children add significant information? An African setting. 31 Postgraduate Course and 45th Annual meeting of European Society of Paediatric Radiology (EPR), Edinburgh. *Pediatr Radiol* 2008;38(Suppl 2):S533.
58. Bosch-Marcet J, Serres-Creixams X, Zuasnahar-Cono A, et al. Comparison of ultrasound with plain radiography and CT for the detection of mediastinal lymphadenopathy in children with tuberculosis. *Pediatr Radiol* 2004;4:895–900.
59. Bosch-Marcet J, Serres-Creixams X, Borrás-Perez V, et al. Value of sonography for follow-up of mediastinal lymphadenopathy in children with tuberculosis. *J Clin Ultrasound* 2007;35:118–24.
60. Scheepers S, Andronikou S, Mapukata A, et al. Abdominal lymphadenopathy in children with tuberculosis presenting with respiratory symptoms. *Pediatr Radiol* 2009;39(Suppl 3):S513.
61. Theron S, Andronikou S. Comparing axillary and mediastinal lymphadenopathy on CT in children with suspected pulmonary tuberculosis. *Pediatr Radiol* 2005;35(9):854–8.
62. Gulati M, Venkataramu NK, Gupta S, et al. Ultrasound guided fine needle aspiration biopsy in mediastinal tuberculosis. *Int J Tuberc Lung Dis* 2000;4:1164–8.
63. Andronikou S, Fink AM. Radiation risk in paediatric CT. *S Afr Med J* 2002;92(7):516.
64. Andronikou S. Pathological correlation of CT-detected mediastinal lymphadenopathy in children: the lack of size threshold criteria for abnormality. *Pediatr Radiol* 2002;32(12):912.
65. Karmazyn, Werner EA, Rejaie B, et al. Mesenteric lymph nodes in children: what is normal. *Pediatr Radiol* 35: 774–7.
66. den Boon S, Bateman ED, Enarson DA, et al. Development and evaluation of a new chest radiograph reading and recording system for epidemiological surveys of tuberculosis and lung disease. *Int J Tuberc Lung Dis* 2005;9:1088–96.